NASA
Technical
Paper
2141

August 1983

Effect of Strain Isolator Pad Modulus on Inplane Strain in Shuttle Orbiter Thermal Protection System Tiles

James Wayne Sawyer

NASA

25th Anniversary
1958-1983

NASA Technical Paper 2141

1983

Effect of Strain Isolator Pad Modulus on Inplane Strain in Shuttle Orbiter Thermal Protection System Tiles

James Wayne Sawyer
Langley Research Center
Hampton, Virginia

NASA
National Aeronautics and Space Administration

Scientific and Technical Information Branch

SUMMARY

An investigation was conducted on the thermal protection system (TPS) used on the Space Shuttle orbiter to determine inplane strains in the reusable surface insulation (RSI) tiles under simulated flight loads. Also, the effects of changes in the strain isolator pad (SIP) moduli on the strains in the tile were evaluated. To analyze the SIP/tile system, it was necessary to determine the material properties of the densified layer of the tile. Thus, tests were conducted to determine inplane tension and compression modulus and inplane failure strain for the densified layer of the two types of tiles, denoted LI-900 and LI-2200, used on the Shuttle.

The test results show that densifying the LI-900 tile material increases the modulus by a factor of 6 to 10. The densified region extends into the material approximately 0.10 in. and has an irregular boundary. This irregular boundary and variations in the distribution of silica throughout the densified material result in large variations in measured modulus values. Densifying the LI-900 tile reduces the failure strain of the material by approximately 50 percent. For the LI-2200 tile, densification results in a more uniform material.

Analysis of the densified LI-900 RSI tile/0.160-in-thick SIP system shows that the inplane strains in the tiles, even for the more highly loaded tiles, are approximately 2 orders of magnitude lower than the inplane failure strain of the tile material. Calculations show that most of the LI-900 tiles on the Shuttle could be mounted on a SIP with tensile and shear stiffnesses 10 times those of the present SIP without inplane strain failure in the tile. A stiffer SIP may have better static and fatigue strength, which might improve the life of the SIP/tile system.

INTRODUCTION

The thermal protection system (TPS) used for high-heating areas of the Space Shuttle orbiter is composed of arrays of reusable surface insulation (RSI) tiles. The tiles are composed of fibrous silica, which is relatively brittle and has a low coefficient of thermal expansion. Because of the differences in the coefficient of thermal expansion between the tiles and aluminum, the tile cannot be bonded directly to the aluminum skin of the orbiter. The tiles are bonded to a fibrous nylon felt strain isolator pad (SIP) which is, in turn, bonded to the aluminum skin. Studies have shown (ref. 1) that densifying the faying surface of the tile significantly improves the static strength of the tile/SIP system. However, fatigue tests (see ref. 2) have shown that cyclic loading results in the SIP extension increasing with each cycle until failure due to separation or excessive elongation of the SIP occurs at a relatively low number of cycles. Improvements in the fatigue life of the SIP/tile system require a change in the SIP material. Attempts to modify the present material or to develop a new SIP with improved static and fatigue strength would most likely result in a stiffer material, which would induce higher strains in the tile and could induce tile failure.

The current investigation was conducted to analyze the SIP/tile system under typical flight load conditions and to evaluate the effects of increasing SIP stiffness on the induced strain in the tile. To analyze the SIP tile system, however, it was necessary to measure the extensional modulus of the densified layer of the RSI tiles. This report includes a description of the test setup and instrumentation developed to measure the inplane tension and compression moduli and inplane failure strains for both types of RSI tiles used on the Shuttle orbiter (commonly referred to as LI-900 and LI-2200 tiles). The measured properties were used with an existing nonlinear structural analysis computer program to determine what effect changes in SIP stiffness would have on the induced strains in the tiles. Although modulus measurements were made for both the LI-900 and LI-2200 tiles, the analysis was limited to the LI-900 tile system, since it is used on the larger portion of the orbiter and has a shorter fatigue life.

ANALYTICAL MODEL

The SIP/tile system was analyzed for loads and substructure deformations typical of those expected on the Shuttle orbiter for the highly loaded tiles. The analytical procedure is presented in reference 3, and a sketch of the analytical model is shown in figure 1. The model consists of a 2-in-thick tile attached to the substructure through a 0.160-in-thick SIP. The tile has a 0.01-in-thick glass coating on the top and sides, but the effects of the coating on the tile sides are neglected. The aerodynamic loads on the tile are represented by a 250-lb tension load offset from the tile center by a 0.5-in. moment arm. The transverse substructure deformation was assumed to be a sine wave with a specified period and a peak-to-peak amplitude of 0.015 in. Calculations were made for different periods so that the substructure was deformed in one, two, three, and four half-waves. The inplane substructure deformation was assumed to be a 0.2-percent linear stretching (yield strain) of the substructure added to a 0.36-percent uniform thermal expansion obtained with a temperature increase of 280°F (from 70°F to 350°F maximum substructure temperature).

The analysis presented in reference 3 considers the tile as an elastic deep beam attached to a nonlinear elastic material (SIP) which, in turn, is attached to the substructure. The beam analysis includes the influence of transverse shear deformations. Inplane strains in the tile were calculated at the glass coating and at the tile/SIP interface for both densified and undensified tiles. The modulus values used in the analysis for the undensified tile and the glass coating on the tile were obtained from reference 4 and are 2.5×10^4 psi and 4×10^6 psi, respectively. The modulus values used for the densified tile layer were obtained as discussed in the following section. SIP material property data used in the analysis are based on a third-order polynomial fit to the experimental stress-strain results presented in references 5 and 6. The third-order stress-strain curves used in the analysis are compared with the experimental data in figure 2. The stress-strain curves used to approximate a stiffer SIP are also shown in figure 2 and are discussed in a subsequent section.

MEASUREMENT OF MODULUS AND FAILURE STRAIN OF DENSIFIED LAYER OF TILE

The test program was conducted to obtain material property data needed to complete the strain analysis of the LI-900 tile system. For completeness of the property data, modulus measurements were also made for the densified LI-2200 tiles. The LI-2200 tile data were not used in the analysis; however, these data have been included in the appendix. They are referred to only as needed to clarify the discussion for the LI-900 tile tests. The test procedure used to obtain the LI-2200 tile data was identical to that used for the LI-900 data.

Specimens

Test specimens used in this investigation were machined from tiles that were made for the Shuttle orbiter but rejected due to dimensional inaccuracies. All the tiles were rectangular parallelepipeds approximately 6.0 in. square by 2.0 in. thick. Several specimens were obtained from each tile. The specimens were made by first rough cutting the tiles into plates of different thicknesses and then sanding the plates to the final thickness. Three to five control specimens were cut from each plate with a precision diamond cutter. The remainder of each plate was densified on one or both sides using the same procedure as that used on the tiles applied to the Shuttle orbiter. The tiles were densified by coating the surface with a mixture of colloidal silica and silica slip (a mixture of small particles of silica and water). After the plates were densified, the sides of the plates were trimmed, and test specimens were cut from each plate with a diamond cutter. Each specimen was numbered so that the tile and the plate from which it was cut could be identified.

Specimen dimensions and orientation with relationship to the tile are shown in figure 3. Specimens with a nominal thickness of 0.25, 0.38, 0.50, and 0.75 in. were tested. A photograph showing a typical specimen of each thickness is shown in figure 4. A photograph of the densified and undensified tile surfaces is shown in figure 5. The ends of the specimens show discolorations due to spillage of the densifying solution on the end of the plate. The width and thickness of each test specimen were measured at three locations along the length. The average values were used in the data analysis and are given in tables I and II.

The effective thickness of the densified layer was determined from photomicrographs of specimen cross sections. A typical photomicrograph is shown in figure 6. The depth of penetration of the densifying material is irregular but is approximately 0.10 in. Microscopic inspection also indicates that the amount of silica in the densified layer varies with distance from the tile surface. The larger particles of silica are trapped near the surface of the tile with the particle size decreasing with distance from the tile surface. The irregular nature of the inner edge of the densified layer and variations in silica distribution suggest that the effective properties of the densified layer may have large variations.

Test Procedures

Tests were conducted using the four-point beam-bending method shown by the sketch in figure 7. Deflection measurements were made at the two loading points and at the center of the beam using three cantilever beam gages as shown in figure 8. These gages were fabricated from stainless steel shim stock 0.008 in. thick, 0.25 in. wide, and 3.75 in. long. They were clamped in a steel fixture, and the distance from the clamp to the point of contact with the test beam was 1.8 in. A strain gage was applied 0.14 in. from the clamp on each side of the cantilever beam gage. An average of the measurements from the two back-to-back strain gages on each cantilever beam was used to determine the deflection of the test beam. The length of the cantilever beam and the thin shim stock from which it was fabricated result in a deflection gage with a very low force deflection ratio; therefore, the deflection gage has an insignificant effect on the data recorded for the test specimens.

Tests were conducted on specimens with a densified layer on one side only and on specimens with the densified layer on both sides. Most specimens were tested several times to approximately 60 percent of the failure load before being loaded to failure. The specimens were rotated 180° between tests so that the densified layer or layers were alternately tested in tension and compression. All tests were conducted using a 500-lb-capacity load frame which incorporated a 50-lb-capacity load cell to measure the applied load. The specimens were loaded at the constant displacement rate of 1.3 in. per minute. A photograph of the test setup is shown in figure 9. The data from the deflection gages and the load cell were recorded using a digital data acquisition system. The calibration of the deflection gages and load cell was checked at the beginning of each day of testing.

Data Analysis

Load-deflection curves were obtained for each of the test specimens and were used in conjunction with beam theory to calculate an effective modulus of elasticity for each of the specimens. For a beam loaded at four points as shown in figure 10, the maximum deflection of the beam occurs at the beam center and when referenced to the point of load application is given as follows:

$$y_{max} = \frac{Ps\ell^2}{8EI} \tag{1}$$

where P, s, and ℓ are defined in figure 10, E is the modulus of elasticity, and I is the moment of inertia about the neutral axis. For an undensified beam, the neutral axis is assumed to lie at the centroid of the cross section; therefore, all the terms in equation (1) are known or can be measured except the tile modulus. Therefore, equation (1) can be used directly with the measured load-deflection results to determine the undensified beam modulus. For the densified beam, the neutral axis is displaced from the centroid of the cross section as shown in figure 10. For this case, EI is given by the following expression:

$$EI = E_b \frac{bh^3}{12} + E_b bh\left(\bar{y} - \frac{h}{2}\right)^2 + \frac{bE_a t^3}{12} + E_b bt\left(h + \frac{t}{2} - \bar{y}\right)^2 \tag{2}$$

where h, t, b, and $\bar{y}$ are as defined in figure 10, E_a is the modulus of the densified layer, E_b is the modulus of the undensified layer, and

$$\bar{y} = \frac{E_b h^2 + 2E_a t(h + t/2)}{2(E_b h + E_a t)} \tag{3}$$

Using the measured modulus value for the undensified layer, all the quantities in equations (1), (2), and (3) are known or can be measured or estimated except the modulus of the densified layer, which can be calculated from equation (3). The calculated moduli were used with the elastic stress-strain relationships to calculate the failure strains for both the densified and undensified materials.

RESULTS AND DISCUSSION

Measured Modulus and Failure Strains of Densified Tile Material

Evaluation of modulus.- Results for a typical densified tile specimen with the densified layer loaded in tension are shown in figure 11. Measured load-deflection results are shown for displacements at the center of the beam and in the regions of load application. The curves are irregular because they were plotted from digitized data with straight lines connecting the data points.

The slope of the load-deflection curve for the center of the beam is required to calculate the effective modulus of the densified layer. The load-deflection curve for the center of the beam is obtained by subtracting the average of the deflections at the load application points from the deflection at the center of the beam. Typical load-deflection curves at the center of several 0.38-in-thick densified and undensified specimens are shown in figure 12. The differences in slope between densified and undensified specimen results are evident in figure 12. The agreement between results for specimens of the same type indicates the consistency of the data. The slopes used in the calculations were obtained from a linear least-squares fit of the test data.

The thickness of the densified layer is also needed to calculate the effective modulus of the densified material, and estimates were made from photomicrographs of the tile cross section. The test data were analyzed to examine the effect of assumed thickness of the densified layer on the modulus of the densified material. Typical results are presented in figure 13, where the effective modulus of the densified material is shown as a function of the assumed thickness of the densified layer. The curves shown were obtained from the measured load-deflection data for specimens with the indicated thicknesses. The modulus results are least sensitive to the assumed thickness of the densified material at a value of about 0.10 in. This is the same value obtained from examination of the photomicrographs of the cross section and, therefore, it was used to reduce the test data. The difference in modulus ratio with specimen thickness shown in figure 13 is within the scatter of data obtained for a single specimen (see table II) and should not be interpreted as a specimen thickness effect.

Summaries of test results are given in table I for the undensified tiles and in table II for the densified tiles. Specimen dimensions and identification number are given along with the calculated modulus or modulus ratio and failure strain. The average and standard deviation of the modulus are also given for each plate. The failure strains are discussed in the next section.

Multiple tests were run on some specimens to assess the repeatability of the results. For example, eight tests were run on undensified specimen number 1101 (table I). The resulting modulus values for the specimen were within ±6 percent of the average. Eight tests were also run on the densified specimen number 1107 (table II). The resulting modulus ratios were within ±24 percent of the average. The repeatability of the test results shown is typical for both the densified and undensified tile specimens. The repeatability of results shown in the appendix for the LI-2200 tiles generally indicates less scatter than that obtained for the LI-900 tiles. Since the test technique was identical, the more consistent results for the LI-2200 tile tests and the undensified LI-900 tile tests suggest that the large variations obtained for the LI-900 densified tiles are largely due to the wide variations in the densified layer thickness and the specimen being located in a slightly different position for each test.

A summary of the modulus and failure strain results for both densified and undensified tiles is shown in table III. The undensified tiles have an average modulus of elasticity that varies between 20 500 psi and 27 200 psi, which is a variation of ±14 percent from the average for the three tiles tested. For tile number 1, the average modulus value for each of the three plate thicknesses tested was within ±7 percent of the average for that tile. However, all the tile data fall within the results presented in reference 4 for the same material.

Modulus data for the LI-900 densified tiles are shown (table III) normalized by the modulus of the undensified material obtained from tests on the same plate. Large variations in modulus ratio for the densified material are indicated. The densified layer in tile 1 has an average modulus approximately 10 times the undensified material modulus, whereas for tiles 2 and 3, the average modulus of the densified layer is slightly less than 6 times the modulus for the undensified material. Relatively large variations in modulus values were also obtained between specimens for densified layers from the same tile (see table II). For example, the densified layer on tile number 1 has an indicated minimum modulus of 5.6 and maximum modulus of 16.5 times the modulus of the undensified tile material. The wide variations indicate that the densification process results in a densified layer with widely varying modulus properties. The modulus values do not show any significant differences due to the densified layer being loaded in tension or compression.

Evaluation of failure strain.- Failure strains for the undensified specimens are given in table I and for the densified specimens in table II. Two strain-at-failure values are given for the specimens densified on one side, whereas only one value is given for the undensified specimens and the specimens densified on two sides. For the specimens densified on one side, the larger strain is in the undensified material, and the smaller strain is in the densified layer. Due to the brittle nature of the failure, it is not possible to tell which strain resulted in failure. However, a comparison of the failure strains obtained from the undensified specimens and the specimens densified on two sides indicates that for the specimens densified on only one side, the failure was probably initiated in the undensified portion of the tile. Average failure strains for the densified and undensified specimens are summarized in table III. Failure strains for the densified layer are approximately one-half the failure strains for the undensified tile material.

Analysis of Tile Strain Levels

The test results for the LI-900 tile material were used with the method described previously to analyze the strain in tiles mounted on 0.160-in-thick SIP as installed on the Shuttle orbiter. Strain levels within the tile are presented for tiles with loads and substructure deformations typical of those in the highly loaded areas of the Shuttle orbiter. The tile/SIP model analyzed is shown in figure 1.

Undensified tile/SIP system.- Typical inplane strain distributions in the undensified tile at the tile/SIP interface and in the glass coating on the tile surface are shown in figure 14(a) and figure 14(b), respectively. Inplane strain is shown as a function of distance along the tile length. The substructure deformations considered are one, two, three, or four half-waves along the tile length. The largest strain in both areas is obtained for the substructure deformed in three half-waves. Since the objective of the analysis is to determine the largest strain within the tile, all subsequent evaluations will be made for the substructure deformed in three half-waves. The maximum strain is approximately 1×10^{-5} in the glass coating and 2×10^{-5} in the tile at the tile/SIP interface. This difference in strain levels is due to the neutral axis being displaced from the centroid of the tile cross-sectional area.

The individual contributions of load and substructure deformation to the strain levels in the tile are shown in figure 15. The loads and deformations applied separately induce low strain levels of opposite signs. The nonlinear characteristic of the tile/SIP system is indicated by the strain levels due to the individual components not adding numerically.

Densified tile/SIP system.- The effect of densification on the strain levels in the tile with a typical load and substructure deformation applied is shown in figure 16. Inplane strains in the tile at the tile/SIP interface (fig. 16(a)) and in the glass coating (fig. 16(b)) are shown as a function of distance along the tile length. The modulus of the densified region was assumed to be 6 times that of the undensified region, and the thickness of the densified region was assumed to be 0.10 in. Densifying the tile substantially reduces the strain level at the tile/SIP interface but only slightly reduces the strain level in the glass coating of the tile. The different reductions in the strain levels are due to the location of the neutral axis in the tile.

Implications for Tile/SIP System

Failure strains for the RSI tiles were measured and discussed previously. The maximum strains expected in both densified and undensified LI-900 RSI tiles on 0.160-in-thick SIP with typical Shuttle loads and substructure deformations were also calculated and discussed. The implications these results may have on the design of future thermal protection systems are discussed in this section.

Measured tensile or compression failure strains for the undensified tiles and densified tiles were approximately 0.0046 and 0.0023, respectively. Data reported in reference 4 for the glass coating on the tile indicate failure strains of 0.001. The calculated maximum strains for tiles with simulated operational loads were approximately 2 orders of magnitude smaller than any of the failure strains indicated above. Thus, the SIP provides more inplane strain isolation than required for the aerodynamic loads and substructure deformations expected. Increasing the stiffness of the SIP could improve the static and fatigue characteristics of the tile/SIP system but could also increase the strain levels in the tile. Thus, it is of interest to determine how changes in SIP properties affect the maximum strain levels in the tile.

The effects of SIP properties on the maximum strain levels in the tile at the SIP/tile interface and in the glass coating of the densified tile are shown in figure 17. Maximum strain levels are shown for variations in the SIP tensile and shear modulus ratios from 1 to 10 times those of the current 0.160-in-thick SIP material. Since the current SIP has nonlinear tensile and shear properties, the tangent modulus varies with the stress or strain level. For the variations in modulus ratios presented in figure 17, the SIP stress-strain relations used in the calculations were obtained from the current 0.160-in-thick SIP properties by increasing the coefficient of the third-order term (C_1 in fig. 2(a) or C_3 in fig. 2(b)) in the equation used to approximate the SIP properties so that the desired secant modulus ratio was obtained at a stress level of 10 psi. The stress-strain relations used in the analysis for the stiffer SIP are shown in figure 2 for modulus ratios of 2, 5, and 10.

The effects of increasing separately the tensile or shear modulus of the SIP are shown respectively by the solid and long-dashed lines in figure 17. Increasing the tensile modulus results in a moderate increase in the strain level in the tile at both locations indicated. For the range of variations in shear modulus values shown, changing the shear modulus has almost no effect on the strain levels.

Since the shear and tensile properties for most practical materials are related, the effects of simultaneously increasing the shear and tensile modulus ratios by equal amounts are also shown in figure 17 by the short-dashed lines. For the standard 0.160-in-thick SIP, the maximum strain at the tile/SIP interface is 2×10^{-5}, and in the glass coating, it is 1×10^{-5}. Increasing both the shear and tensile stiffness of the SIP by a factor of 10 results in a maximum strain in the tile at the SIP/tile interface of 16.5×10^{-5} and in the glass coating of the tile of 8.5×10^{-5}. For the range of stiffnesses considered, simultaneously increasing both the tensile and shear moduli of the SIP results in only slight additional strain in the tile over that obtained with only an increase in tensile modulus.

The strain data presented in the previous figures were obtained for 2.0-in-thick tiles. Larger strain levels could be obtained for thinner tiles subjected to the same loads and substructure deformations. Thus, figure 18 shows the maximum strain in the tile as a function of thickness for tiles subjected to the loads and substructure deformations discussed previously. Curves are presented for the tiles on both the standard 0.160-in-thick SIP and on 0.160-in-thick SIP that has shear and tensile moduli 10 times those of the standard SIP. The failure strains for the tile glass coating and the densified tile material are also indicated on the figure.

From the results presented, it can be seen that tiles bonded to the stiffened SIP have significantly higher strains than tiles bonded to the standard SIP and that the difference in strain increases as the tile thickness is reduced. However, even for a tile with a thickness of 0.50 in., the maximum strains are less than 50 percent of the average material failure strains. In view of these results and the conservative nature of the assumed loading conditions, an improved SIP with tensile and shear stiffnesses up to 1 order of magnitude larger than the present SIP material should be acceptable without causing inplane failure strains in tiles with a thickness greater than 0.50 in. For specific areas of the Shuttle where the loads and substructure deformations are known to be low or where the tile thicknesses are greater than 1.0 in., even larger increases in the SIP stiffness may be acceptable without causing inplane failure strains in the tile.

CONCLUDING REMARKS

An investigation has been conducted on the thermal protection system used on the Space Shuttle orbiter to determine the strains in the reusable surface insulation (RSI) tiles under simulated maximum flight loads. Also, the effects of changes in the strain isolator pad (SIP) moduli on the strains in the tile were evaluated. To analyze the SIP/tile system, it was necessary to determine the material properties of the densified layer of the tiles. Thus, tests were conducted to determine the tension and compression material properties for the densified layer of the LI-900 and LI-2200 tiles.

The test results show that densifying the LI-900 tile material increases the modulus by a factor of 6 to 10 over that of the undensified tile material. The densified region extends into the material approximately 0.10 in. and has an irregular boundary. This irregular boundary and variations in the distribution of silica throughout the densified material result in the large variation in the measured modulus values. Densifying the LI-900 tile material reduces the failure strain by approximately 50 percent. For the LI-2200 tile material, densification has a much more uniform effect on the material properties.

Analysis of the LI-900 RSI tile/0.160-in-thick SIP system shows that the inplane strains in the tiles, even for the more highly loaded tiles, are approximately 2 orders of magnitude lower than the inplane failure strain of the tile material. Calculations show that most of the LI-900 tiles on the Shuttle could be mounted on a SIP with tensile and shear stiffnesses 10 times those of the present SIP without inplane strain failure in the tile. A stiffer SIP may have better static and fatigue strength, which might improve the life expectancy of the SIP/tile system.

Langley Research Center
National Aeronautics and Space Administration
Hampton, VA 23665
June 27, 1983

APPENDIX

EXPERIMENTAL TESTS AND RESULTS FOR LI-2200 TILES

The experimental test and analysis procedure used for the LI-2200 tiles is identical to that used for the LI-900 tiles and is described in the body of the report. The thicknesses of the densified layer of the specimens were determined from photomicrographs (see fig. 19) of the cross sections of the specimens and were found to be approximately 0.06 in. The effective modulus of the densified layer is shown in figure 20 to be relatively insensitive to the thickness, especially near the measured value of 0.06 in.

The dimensions of the LI-2200 specimens, the calculated modulus or modulus ratio, and the failure strain are given in tables IV and V for the undensified and densified specimens, respectively. The average and standard deviation of the modulus values are given for each plate. Note that two values of failure strain are given for the densified specimens. These are the strains in the densified and undensified portions of the specimen. The strain that initiates specimen failure cannot be determined from the test results. Since LI-2200 specimens densified on both sides were not tested, the failure strain of the densified material cannot be determined but is at least as large as the strain indicated in table V.

Repeat tests of the same specimen (on both densified and undensified material) show good reproducibility of modulus values, much better than that obtained for the densified LI-900 tile specimens. Since the test technique was identical for the two tile materials, the more repeatable results for the LI-2200 tests show that the properties are more consistent for the densified layer in the LI-2200 tiles than in the LI-900 tiles. Tests of the same specimen with the densified layer alternately tested in tension and compression show no significant difference in the tension and compression moduli for the specimens.

A summary of the results for each tile and plate is given in table VI. The average modulus of elasticity for the undensified LI-2200 tile material varies between 67 900 psi and 77 800 psi, which is a ±9 percent variation from the average for the two tiles tested. These data fall within the range of results presented in reference 4 for the same material. The average modulus of the densified layer is approximately 3 to 4 times the modulus of the undensified material. Failure strains are approximately 0.0038 for the undensified material but were not determined for the densified layer, as noted previously.

REFERENCES

1. Cooper, Paul A.; and Holloway, Paul F.: The Shuttle Tile Story. Astronaut. & Aeronaut., vol. 19, no. 1, Jan. 1981, pp. 24-34, 36.

2. Sawyer, James Wayne; and Cooper, Paul A.: Fatigue Properties of Shuttle Thermal Protection System. NASA TM-81899, 1980.

3. Stein, Manuel; and Stein, Peter A.: A Solution Procedure for Behavior of Thick Plates on a Nonlinear Foundation and Postbuckling Behavior of Long Plates. NASA TP-2174, 1983.

4. Materials and Processes Group, Shuttle Eng.: Materials Properties Manual - Volume 3: Thermal Protection System Materials Data. PUB 2543-W REV 5-79, Rockwell International, May 1979.

5. Sawyer, James Wayne: Effect of Load Eccentricity and Substructure Deformations on Ultimate Strength of Shuttle Orbiter Thermal Protection System. NASA TM-83182, 1981.

6. Sawyer, James Wayne; and Waters, William Allen, Jr.: Room Temperature Shear Properties of the Strain Isolator Pad for the Shuttle Thermal Protection System. NASA TM-81900, 1981.

TABLE I.- SPECIMEN DIMENSIONS AND TEST RESULTS FOR UNDENSIFIED LI-900 TILES

Test no.	Specimen identification no.[a]	Width, in.	Thickness, in.	Calculated modulus, E, psi	Failure strain
1	1101	0.4946	0.2366	21 400	
2				23 000	
3				21 700	
4				22 500	
5				23 500	
6				21 300	
7				23 800	
8				22 400	0.0045
9	1102	0.4950	0.2391	21 900	
10				22 100	
11				22 400	
12				22 700	0.0046
13	1103	0.4933	0.2368	22 000	
14				22 400	
15				22 300	
16				22 800	0.0050
	Average			22 400	
	Standard deviation			700	
45	1201	0.4947	0.3741	25 700	
46				25 200	
47				24 800	
48				24 000	0.0046
49	1202	0.4932	0.3692	23 600	
50				24 000	
51				24 500	
52				23 600	0.0045
53	1203	0.4934	0.3677	22 300	
54				21 500	
55				22 300	
56				21 600	0.0049
	Average			23 600	
	Standard deviation			1 400	

[a]Description of specimen identification number:

1101

- two-digit specimen number
- plate number
- tile number

TABLE I.- Concluded

Test no.	Specimen identification no.[a]	Width, in.	Thickness, in.	Calculated modulus, E, psi	Failure strain
84	1301	0.4944	0.4970	24 700	
85				25 400	
86				26 200	
87				26 200	0.0040
88	1302	0.4941	0.4938	26 300	
89				23 700	
90				25 400	
91				24 000	0.0046
92	1303	0.4921	0.4951	25 400	
93				27 300	
94				27 000	
95				25 700	0.0042
	Average			25 600	
	Standard deviation			1 100	
121	2101	0.4949	0.7443	25 900	
122				25 600	
123				25 800	
124				29 400	
125	2102	0.4954	0.7453	26 200	
126				26 600	
127				25 100	
128				28 900	
129	2103	0.4978	0.7463	25 900	
130				28 600	
131				28 000	
132				30 100	
	Average			27 200	
	Standard deviation			1 700	
151	3101	0.5012	0.5009	21 000	
152	3102	0.4994	0.5011	20 100	
153	3103	0.4999	0.5003	21 400	
154				21 100	
155	3104	0.5000	0.5013	20 900	
156				20 100	
157	3105	0.5009	0.5014	19 400	
158				19 800	
	Average			20 500	
	Standard deviation			700	

[a] See footnote on page 12.

TABLE II.- SPECIMEN DIMENSIONS AND TEST RESULTS FOR DENSIFIED LI-900 TILES

Test no.	Specimen identification no.[a]	Width, in.	Thickness, in.	Location of densified layer	Modulus ratio, E_a/E_b	Failure strain
17	1104	0.5017	0.2360	Bottom	7.5	
18				Top	7.2	
19				Bottom	7.0	0.0045
20				Top	8.8	.0017
21	1105	0.5020	0.2342	Top	11.4	
22				Bottom	10.7	
23				Top	10.2	0.0042
24				Bottom	10.0	.0016
25	1106	0.5015	0.2364	Top	9.7	
26				Bottom	7.1	
27				Top	9.0	0.0044
28				Bottom	7.3	.0018
29	1107	0.5011	0.2430	Bottom	7.3	
30				Bottom	6.4	
31				Bottom	6.5	
32				Bottom	6.6	
33				Top	8.8	
34				Bottom	6.6	
35				Top	8.4	0.0047
36				Bottom	6.1	.0020
37	1108	0.5017	0.2368	Bottom	8.1	
38				Top	9.1	
39				Bottom	6.8	0.0041
40				Top	7.6	.0017
41	1109	0.5019	0.2379	Top	7.8	
42				Bottom	6.2	
43				Top	8.1	0.0036
44				Bottom	5.6	.0016
Average					7.9	
Standard deviation					1.5	

[a]Description of specimen identification number:

1101
- two-digit specimen number
- plate number
- tile number

TABLE II.- Continued

Test no.	Specimen identification no.[a]	Width, in.	Thickness, in.	Location of densified layer	Modulus ratio, E_a/E_b	Failure strain
57	1204	0.5020	0.3714	Top	7.9	
58				Bottom	9.2	
59				Top	8.6	0.0052
60				Bottom	8.1	.0018
61	1205	0.5019	0.3637	Bottom	7.5	
62				Top	9.1	0.0039
63				Bottom	6.1	.0016
64	1206	0.5022	0.3619	Bottom	9.6	
65				Top	8.5	
66				Bottom	8.0	
67				Top	10.9	
68	1207	0.5108	0.3708	Top	13.2	
69				Bottom	10.5	
70				Top	10.5	0.0050
71				Bottom	8.2	.0017
72	1208	0.5015	0.3640	Top	13.2	
73				Bottom	10.9	
74				Top	13.4	0.0049
75				Bottom	8.8	.0017
76	1209	0.5018	0.3652	Bottom	12.4	
77				Top	12.9	
78				Bottom	8.9	0.0046
79				Top	15.0	.0012
80	1210	0.5020	0.3623	Bottom	9.4	
81				Top	8.6	
82				Bottom	9.5	0.0044
83				Top	12.5	.0013
Average					10.0	
Standard deviation					2.2	

See footnote on page 14.

TABLE II.- Continued

Test no.	Specimen identification no.[a]	Width, in.	Thickness, in.	Location of densified layer	Modulus ratio, E_a/E_b	Failure strain
96	1304	0.5013	0.4885	Bottom	9.4	
97				Top	10.4	0.0032
98				Bottom	9.4	.0011
99	1305	0.5015	0.4921	Bottom	5.7	0.0035
100				Top	7.5	.0013
101	1306	0.5018	0.4900	Top	11.1	
102				Bottom	5.7	
103				Top	9.8	0.0043
104				Bottom	5.7	.0019
105	1307	0.5022	0.4884	Bottom	10.8	
106				Top	8.2	
107				Bottom	7.9	0.0035
108				Top	8.0	.0013
109	1308	0.5621	0.4906	Top	12.5	
110				Bottom	10.8	
111				Top	8.3	0.0037
112				Bottom	7.9	.0014
113	1309	0.5020	0.4890	Bottom	10.9	
114				Top	12.0	
115				Bottom	9.6	0.0035
116				Top	12.9	.0010
117	1310	0.5022	0.4899	Top	16.5	
118				Bottom	14.2	
119				Top	9.3	0.0037
120				Bottom	10.5	.0012
Average					9.8	
Standard deviation					2.6	

See footnote on page 14.

TABLE II.- Concluded

Test no.	Specimen identification no.[a]	Width, in.	Thickness, in.	Location of densified layer	Modulus ratio, E_a/E_b	Failure strain
133	2104	0.4736	0.7498	Top	5.6	
134				Bottom	5.0	
135				Top	4.4	
136				Bottom	7.8	
137				Top	5.2	
138				Bottom	5.8	
139	2105	0.4995	0.7401	Bottom	6.9	
140				Top	7.0	
141	2106	0.5014	0.7442	Bottom	4.2	
142				Top	6.5	
143	2107	0.5012	0.7411	Bottom	5.1	
144				Top	3.6	
145	2108	0.5011	0.7391	Top	4.8	
146				Bottom	6.2	
147	2109	0.5016	0.7392	Top	5.3	
148				Bottom	6.4	
149	2110	0.5014	0.7395	Top	6.5	
150				Bottom	7.5	
	Average				5.8	
	Standard deviation				1.2	
161	3106	0.5000	0.7433	Top & bottom	5.4	
162					5.2	
163					3.8	0.0024
164	3107	0.5016	0.7477	Top & bottom	4.6	
165					3.9	
166					3.6	0.0025
167	3108	0.5017	0.7445	Top & bottom	5.2	
168					6.3	
169					4.2	0.0024
170	3109	0.5020	0.7457	Top & bottom	5.1	
171					7.8	
172					4.9	0.0020
173	3110	0.5019	0.7460	Top & bottom	5.3	
174					5.7	
175					4.3	0.0022
176	3111	0.5016	0.7453	Top & bottom	5.9	
177					6.3	
178					4.4	0.0021
179	3112	0.5012	0.7453	Top & bottom	4.8	
180					5.6	
181					3.9	0.0024
	Average				5.1	
	Standard deviation				1.0	

See footnote on page 14.

TABLE III.- AVERAGE MODULUS VALUES AND FAILURE STRAINS OF DENSIFIED AND UNDENSIFIED LI-900 MATERIAL

Tile no.	Plate no.	Nominal specimen thickness, in.	Undensified modulus, psi	Densified modulus ratio, E_a/E_b	Failure strain	
					Undensified	Densified
1	1	0.25	22 400	7.9	0.0047	
	2	.38	23 600	10.0	.0047	
	3	.50	25 600	9.8	.0043	
2	1	0.75	27 200	5.8		
3	1	0.50	20 500	5.1		0.0023

TABLE IV.- SPECIMEN DIMENSIONS AND TEST RESULTS FOR UNDENSIFIED LI-2200 TILES

Test no.	Specimen identification no.[a]	Width, in.	Thickness, in.	Calculated modulus, E, psi	Failure strain
182	4101	0.4936	0.2411	72 000	
183				66 400	
184				66 400	
185				66 100	
186				65 700	
187				67 500	
188				67 700	
189				71 400	
190				70 500	
191				70 300	0.0037
192	4102	0.4943	0.2414	65 100	
193				67 200	
194				65 500	
195				68 500	0.0039
	Average			67 900	
	Standard deviation			2 300	

[a]Description of specimen identification number:

1101
- └── two-digit specimen number
- └── plate number
- └── tile number

TABLE IV.- Concluded

Test no.	Specimen identification no.[a]	Width, in.	Thickness, in.	Calculated modulus, E, psi	Failure strain
224	5101	0.4943	0.3705	73 800	
225				71 900	
226				76 400	
227				75 400	
228				76 000	
229				75 000	
230				77 900	
231				79 800	
232				79 200	0.0039
233	5102	0.4958	0.3734	81 400	
234				78 500	
235				82 800	
236				82 700	0.0037
	Average			77 800	
	Standard deviation			3 400	
261	5201	0.4940	0.4990	78 000	
262				81 100	
263				75 500	
264				76 500	
265				80 000	
266				79 800	
267				72 500	
268				77 500	0.0034
269	5202	0.4945	0.4981	79 500	
270				80 000	
271				71 800	
272				71 700	0.0038
	Average			77 200	
	Standard deviation			3 400	

See footnote on page 19.

TABLE V.- SPECIMEN DIMENSIONS AND TEST RESULTS FOR DENSIFIED LI-2200 TILES

Test no.	Specimen identification no.[a]	Width, in.	Thickness, in.	Location of densified layer	Modulus ratio, E_a/E_b	Failure strain
196	4103	0.5025	0.2363	Top	3.1	0.0033
197				Bottom	2.5	.0022
198	4104	0.5019	0.2386	Bottom	2.9	
199				Top	2.6	
200				Bottom	2.5	0.0034
201				Top	2.7	.0022
202	4105	0.5019	0.2400	Top	2.6	
203				Bottom	2.5	
204				Top	2.6	0.0036
205				Bottom	2.5	.0024
206	4106	0.5018	0.2354	Bottom	2.5	
207				Top	2.6	
208				Bottom	2.2	0.0030
209				Top	2.5	.0020
210	4107	0.5022	0.2380	Top	3.3	
211				Bottom	3.2	
212				Top	3.0	0.0037
213				Bottom	2.8	.0023
214	4108	0.5017	0.2394	Bottom	2.5	
215				Top	2.8	
216				Bottom	2.5	0.0033
217				Top	2.9	.0020
218	4109	0.5020	0.2391	Top	3.2	
219				Bottom	3.0	
220				Top	2.9	0.0036
221				Bottom	2.9	.0022
222	4110	0.5017	0.2400	Bottom	3.7	0.0027
223				Top	3.5	.0015
Average					2.8	
Standard deviation					0.4	

[a]Description of specimen identification number:

1101

two-digit specimen number

plate number

tile number

TABLE V.- Continued

Test no.	Specimen identification no.[a]	Width, in.	Thickness, in.	Location of densified layer	Modulus ratio, E_a/E_b	Failure strain
237	5103	0.5015	0.3658	Top	3.5	
238				Bottom	2.9	
239				Top	3.0	
240	5104	0.5017	0.3657	Bottom	3.6	
241				Top	3.6	
242				Bottom	3.3	0.0041
243				Top	3.6	.0025
244	5105	0.5007	0.3680	Top	3.5	
245				Bottom	3.0	
246				Top	3.0	0.0043
247				Bottom	2.9	.0029
248	5106	0.5017	0.3666	Bottom	3.1	
249				Top	3.2	
250				Bottom	2.6	0.0042
251				Top	3.2	.0027
252	5107	0.5015	0.3680	Top	3.4	0.0036
253				Bottom	3.3	.0023
254	5108	0.5018	0.3661	Top	3.7	
255				Top	3.3	0.0039
256				Bottom	3.1	.0025
257	5109	0.5016	0.3655	Bottom	3.6	
258				Top	3.4	
259				Bottom	3.0	0.0043
260				Top	3.4	.0027
Average					3.3	
Standard deviation					0.3	

See footnote on page 21.

TABLE V.- Concluded

Test no.	Specimen identification no.[a]	Width, in.	Thickness, in.	Location of densified layer	Modulus ratio, E_a/E_b	Failure strain
273	5203	0.5020	0.4963	Top	3.5	
274				Bottom	4.6	
275				Top	3.2	
276				Bottom	3.3	0.0033
277				Bottom	2.9	.0023
278	5204	0.5022	0.4963	Bottom	4.9	
279				Top	3.7	
280				Bottom	4.3	
281				Top	3.8	0.0035
282				Top	3.7	.0023
283	5205	0.4991	0.4974	Top	4.3	
284				Bottom	4.4	
285				Top	4.0	
286				Bottom	4.2	0.0038
287				Bottom	3.4	.0025
288	5206	0.5019	0.4973	Bottom	4.0	
289				Top	3.9	
290				Bottom	4.2	
291				Top	3.7	0.0037
292				Top	3.6	.0024
293	5207	0.5018	0.4971	Top	5.0	
294				Bottom	5.0	
295				Top	4.4	
296				Bottom	4.6	0.0030
297				Bottom	4.4	.0018
298	5208	0.5023	0.4966	Bottom	4.8	
299				Top	3.7	
300				Bottom	4.0	
301				Top	4.6	0.0035
302				Top	4.8	.0020
303	5209	0.5009	0.4959	Top	3.5	
304				Bottom	3.3	
305				Top	3.3	
306				Bottom	3.4	0.0034
307				Bottom	3.1	.0024
Average					4.0	
Standard deviation					0.6	

See footnote on page 21.

TABLE VI.- AVERAGE MODULUS VALUES AND FAILURE STRAINS OF DENSIFIED AND UNDENSIFIED LI-2200 MATERIAL

Tile no.	Plate no.	Nominal specimen thickness, in.	Undensified modulus, psi	Densified modulus ratio, E_a/E_b	Failure strain	
					Undensified	Densified
4	1	0.25	67 900	2.8	0.0038	
5	1	0.38	77 800	3.3	0.0038	
	2	.50	77 200	4.0	.0036	

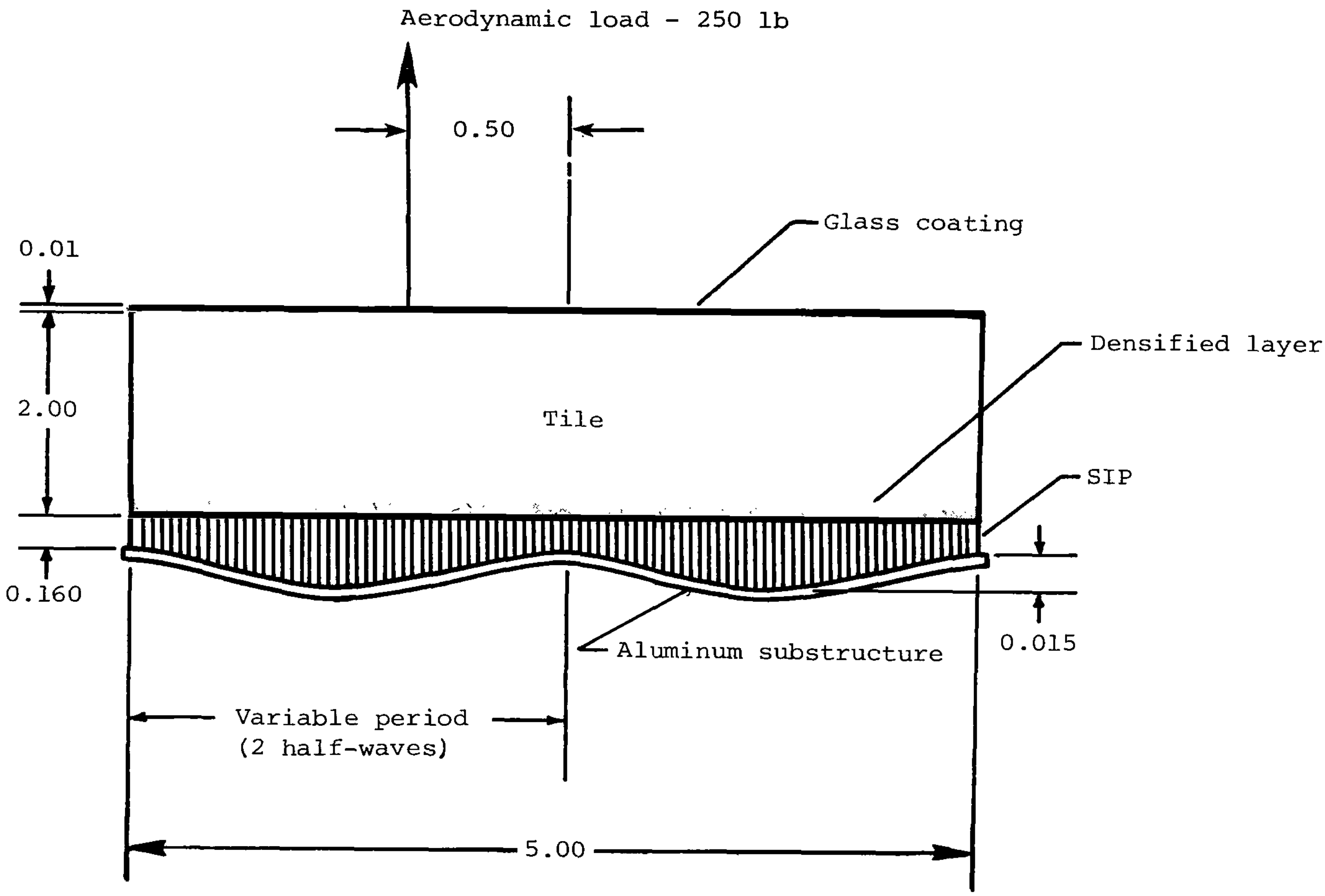

Figure 1.- Description of the tile TPS considered in the analysis. Substructure deformation includes 0.2-percent inplane stretching and 280°F differential temperature thermal expansion. Linear dimensions in inches.

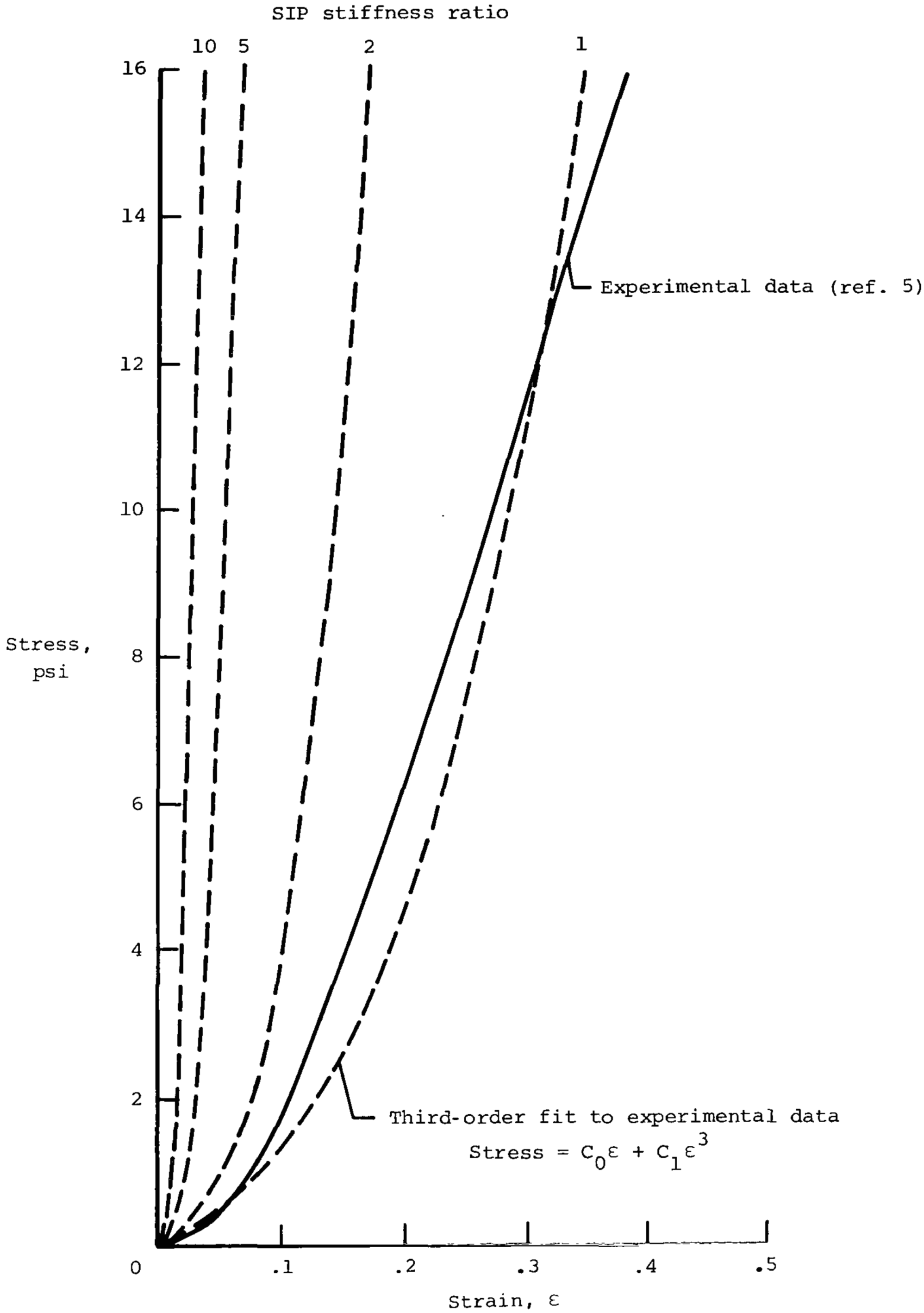

(a) Tensile properties.

Figure 2.- Stress-strain properties for the 0.160-in-thick SIP.

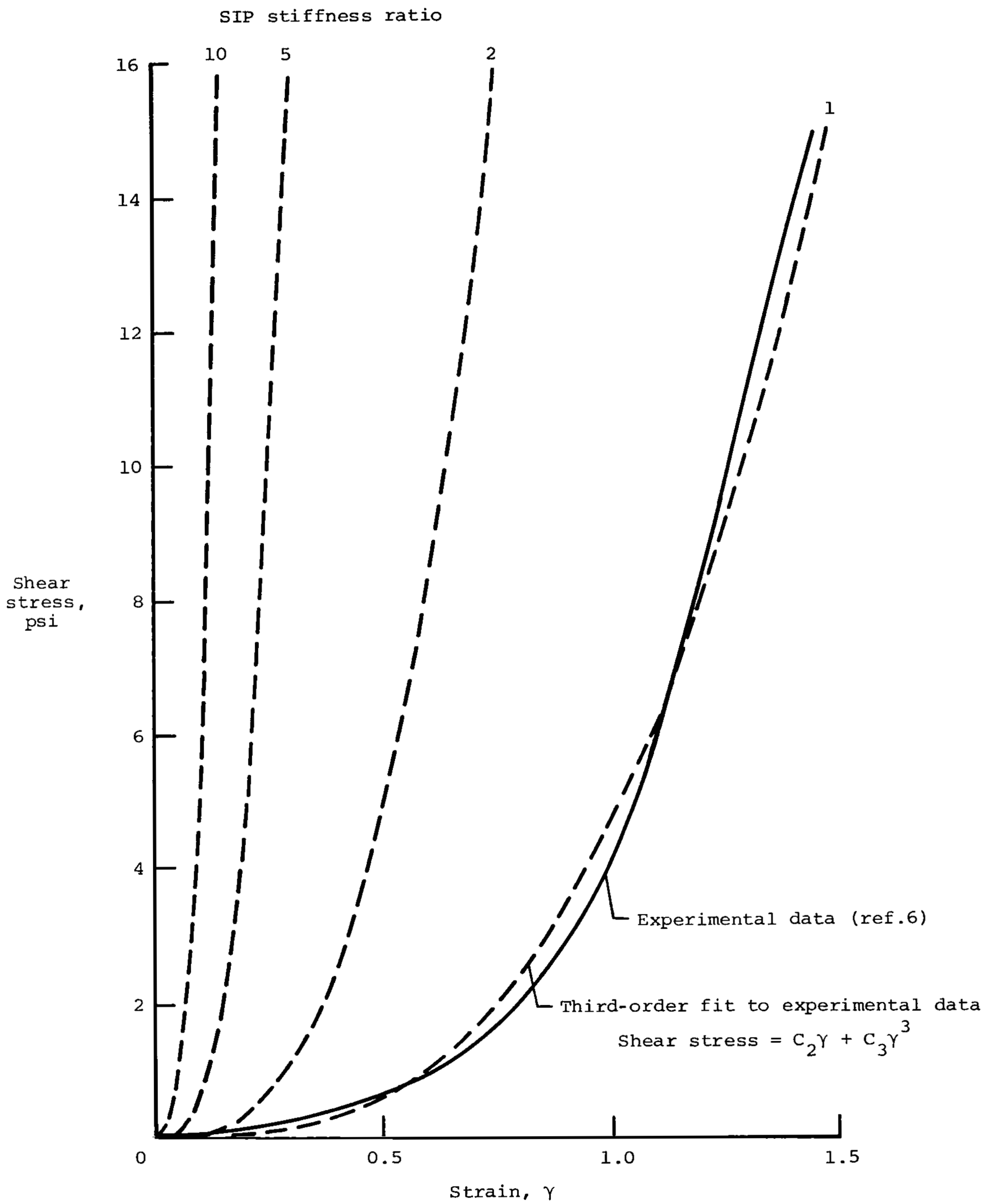

(b) Shear properties.

Figure 2.- Concluded.

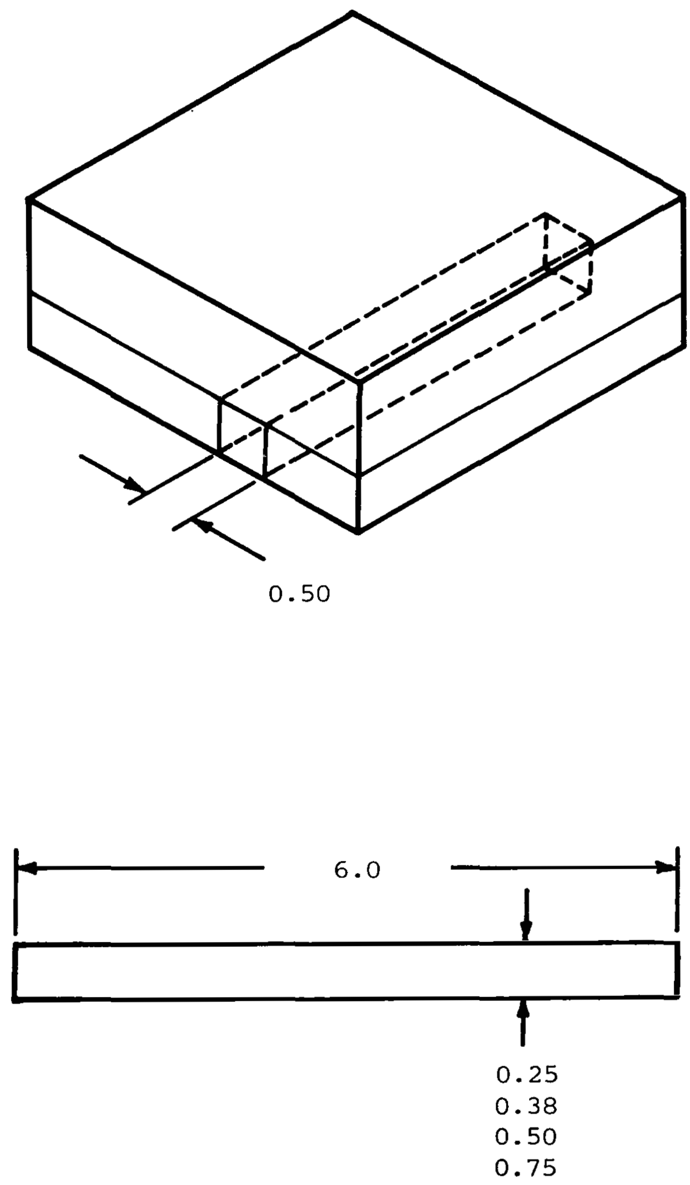

Figure 3.- Specimen dimensions and orientation in tile. Dimensions in inches.

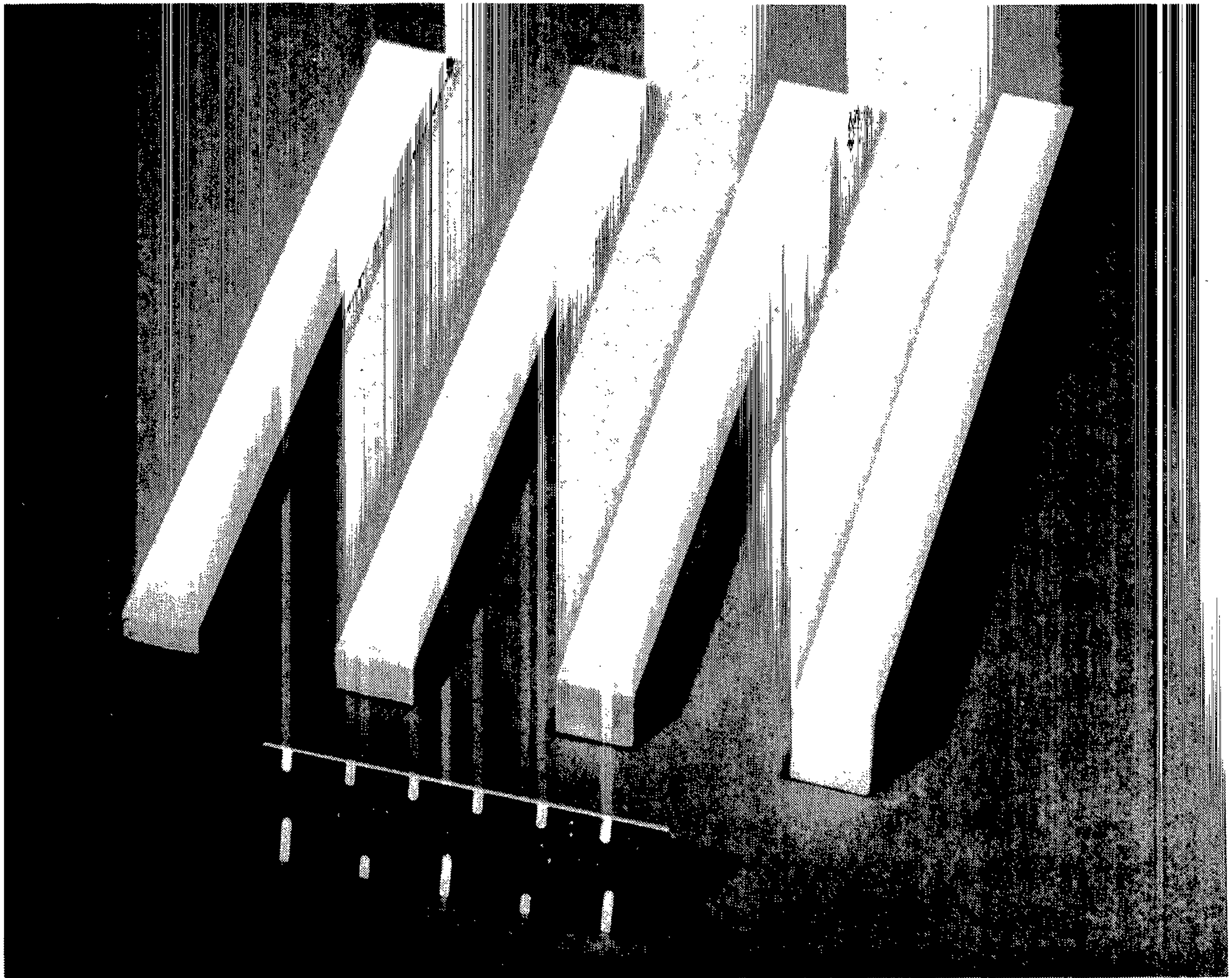

L-83-92

Figure 4.- Photograph of typical test specimens.

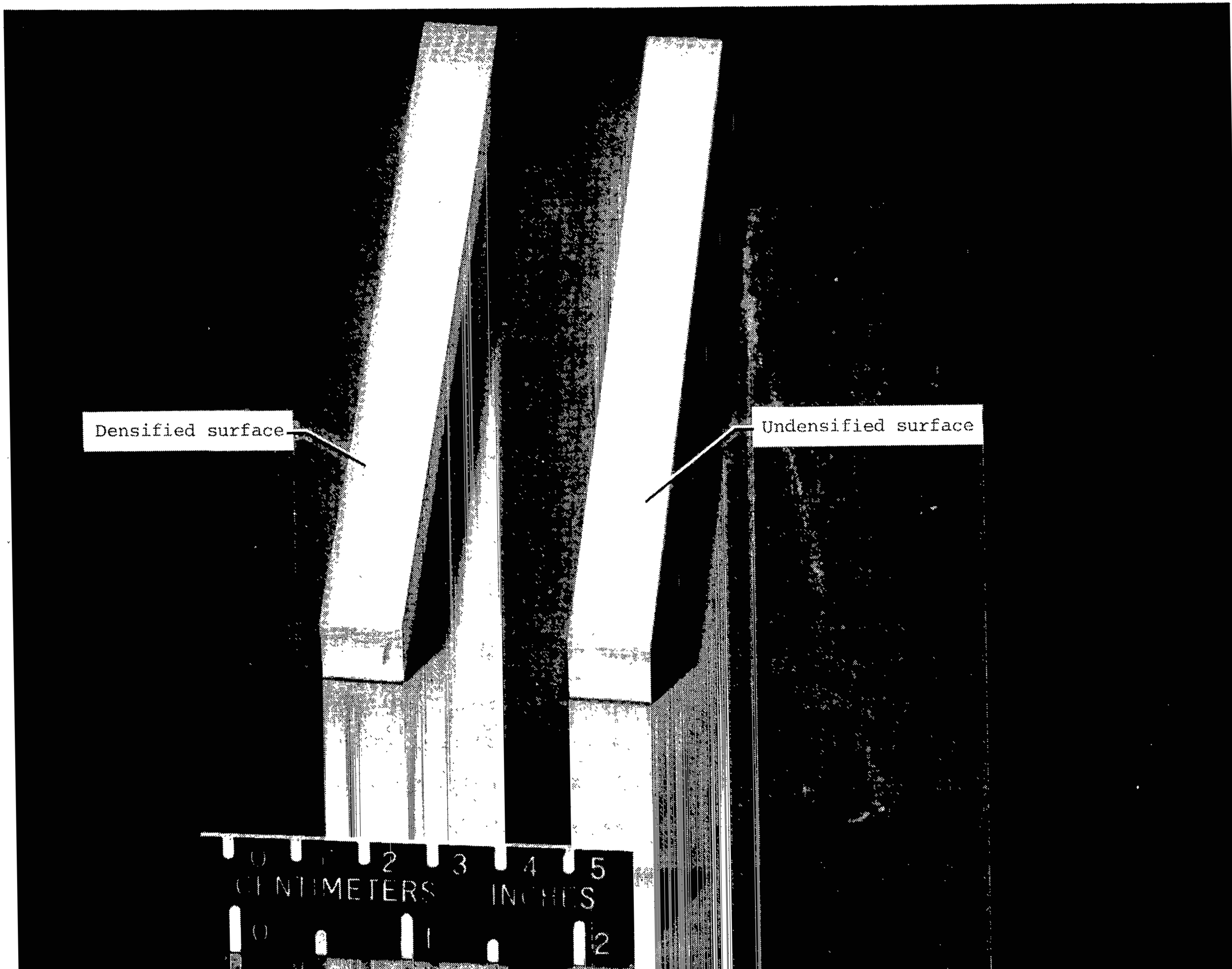

L-81-9921.1

Figure 5.- Photograph of typical densified and undensified tile surfaces.

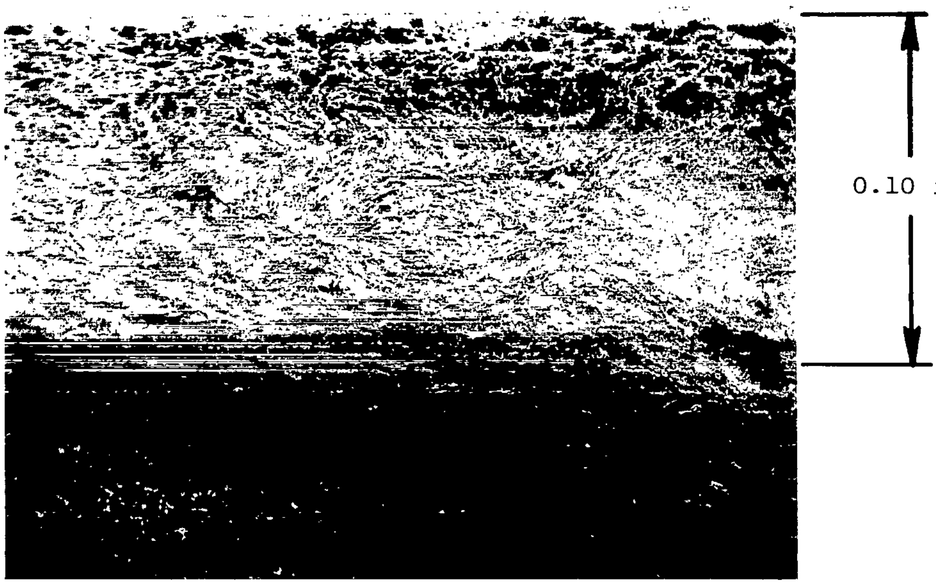

L-83-93

Figure 6.- Photomicrograph of typical cross section of densified LI-900 tile specimen.

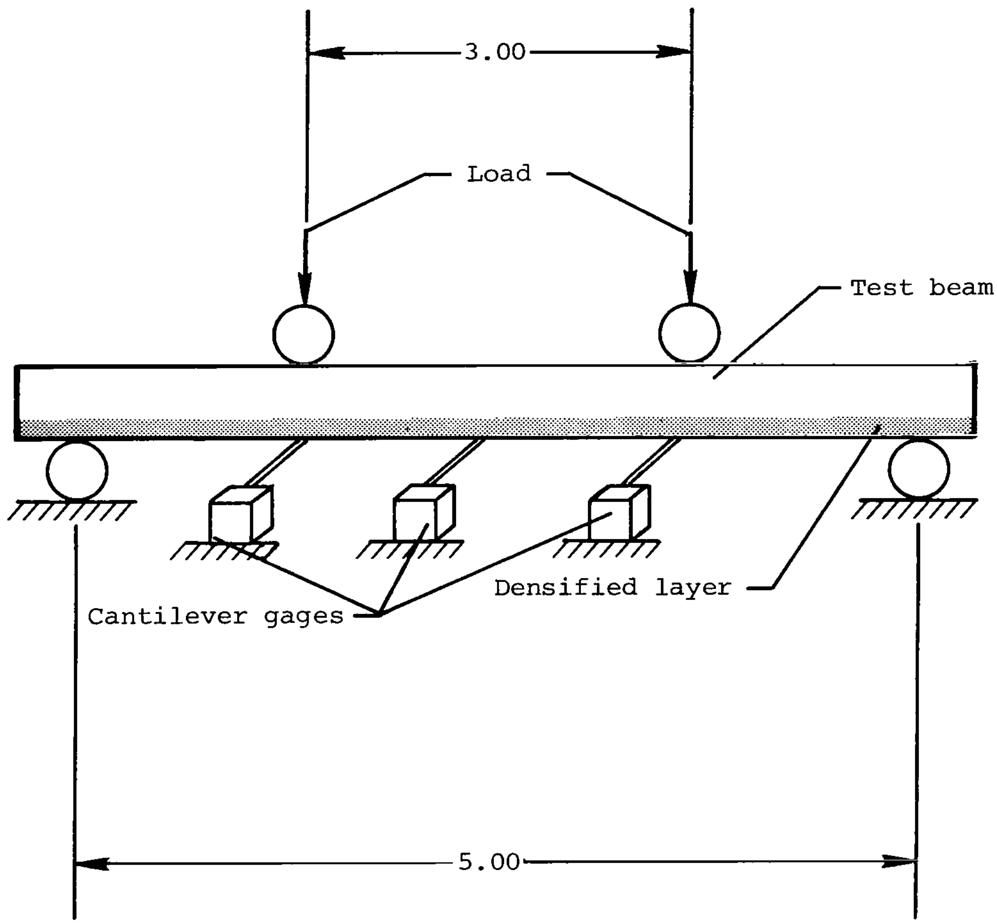

Figure 7.- Sketch of test setup. Dimensions in inches.

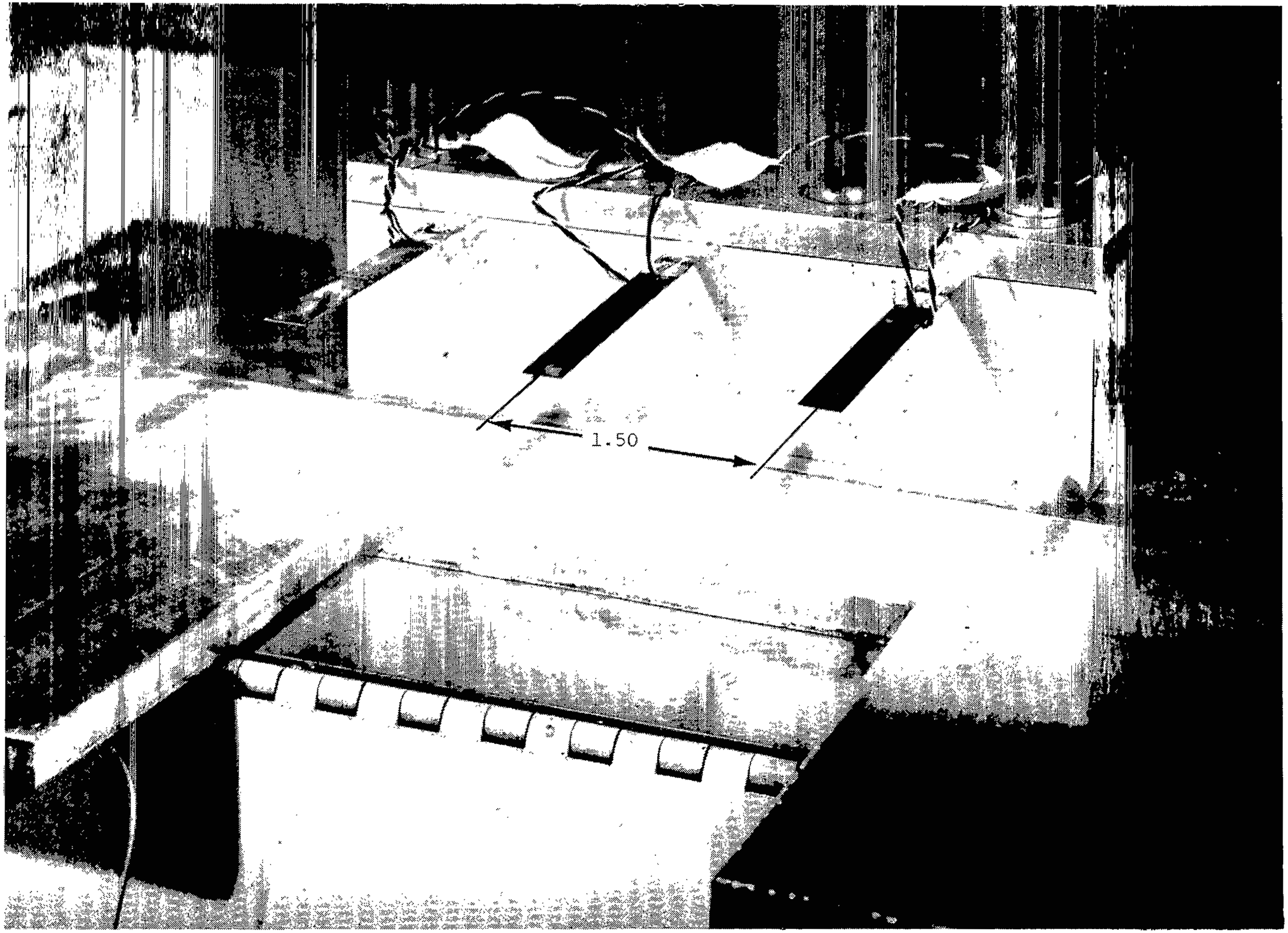

L-81-11380.1

Figure 8.- Cantilever beam gages used to measure deflection of the test specimens. Dimensions in inches.

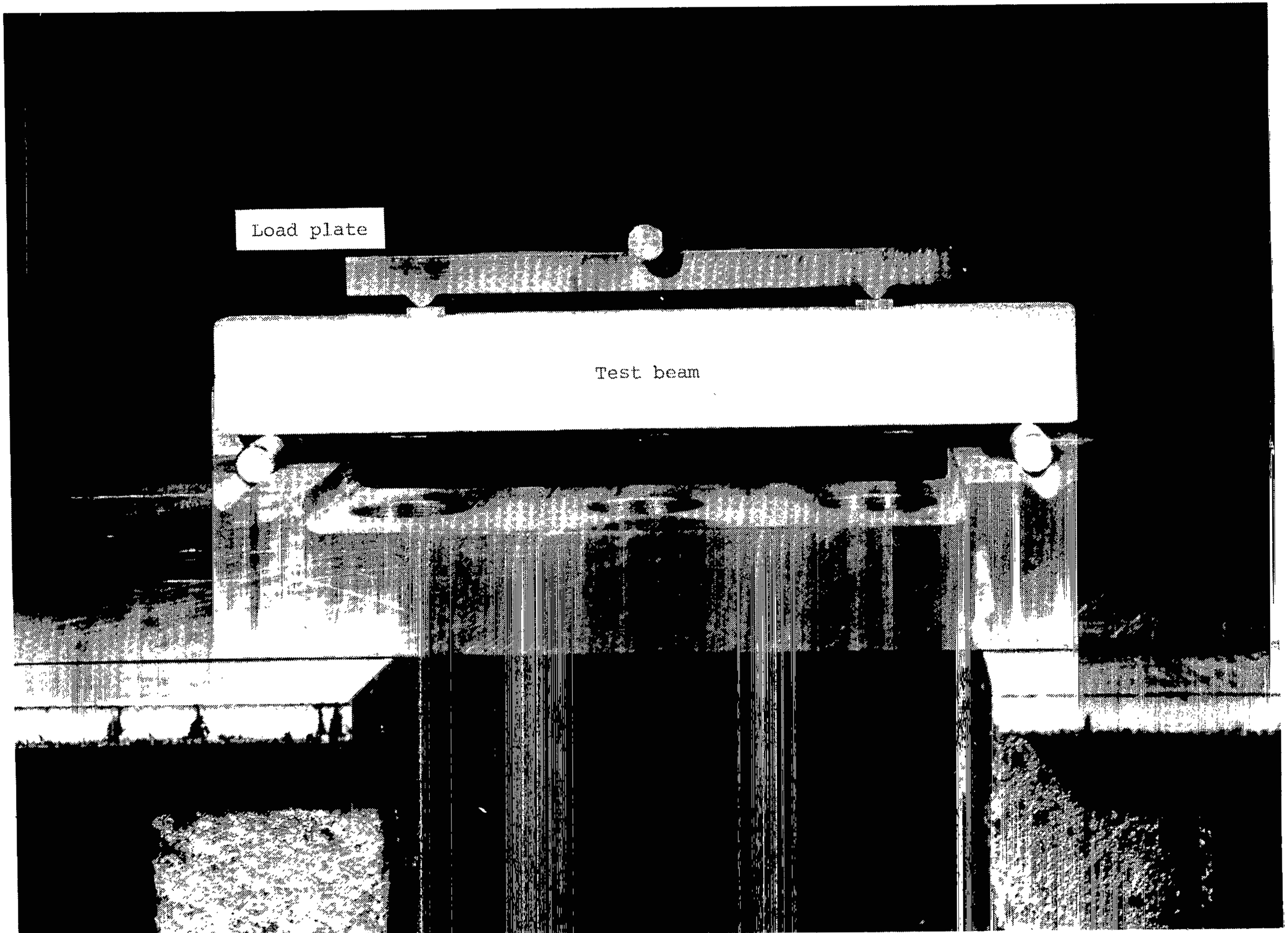

L-81-11379.1

Figure 9.- Photograph of test setup.

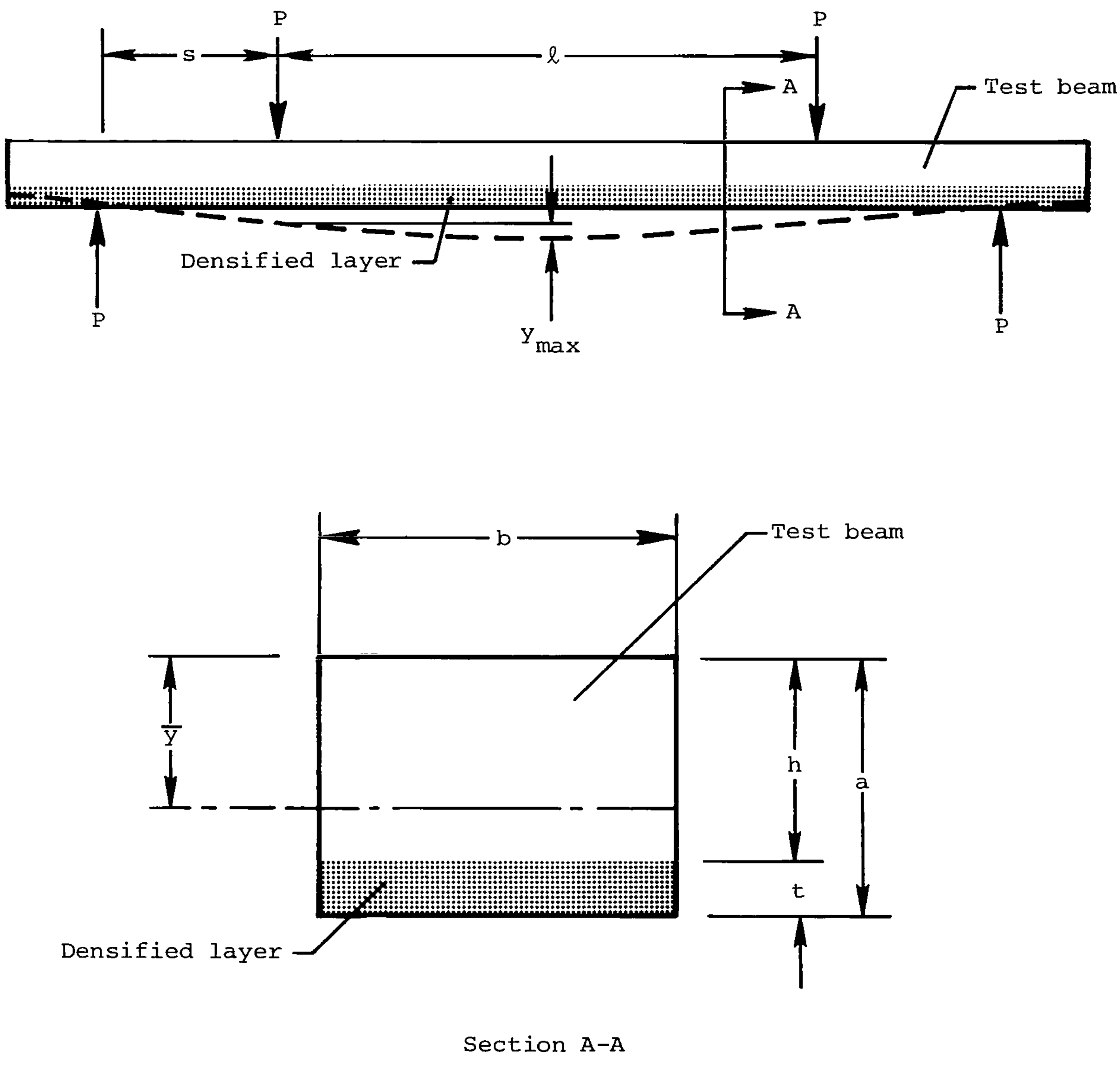

Figure 10.- Sketch of densified beam specimen loaded at four points.

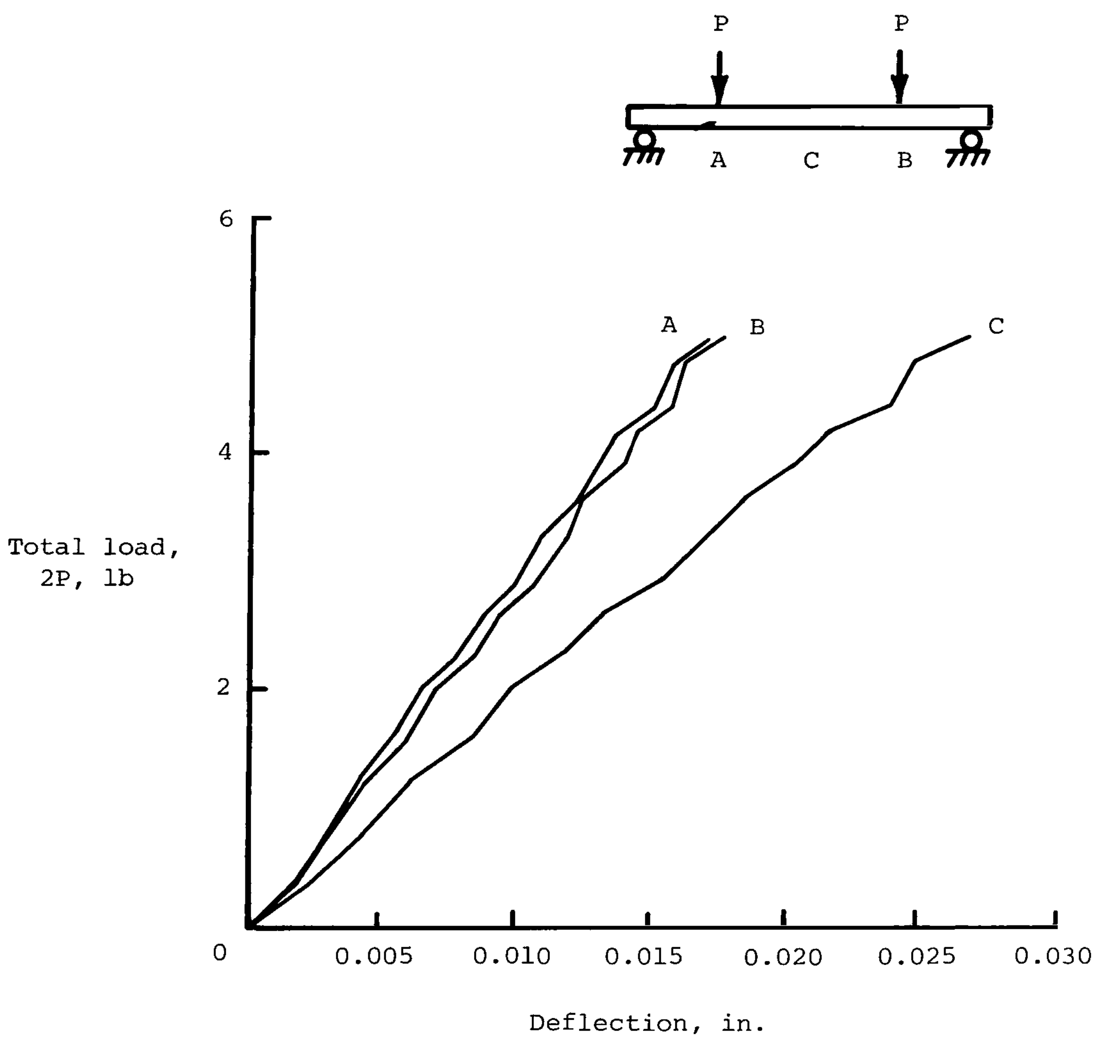

Figure 11.- Typical load-deflection curves for an LI-900 densified tile specimen. Densified material in tension.

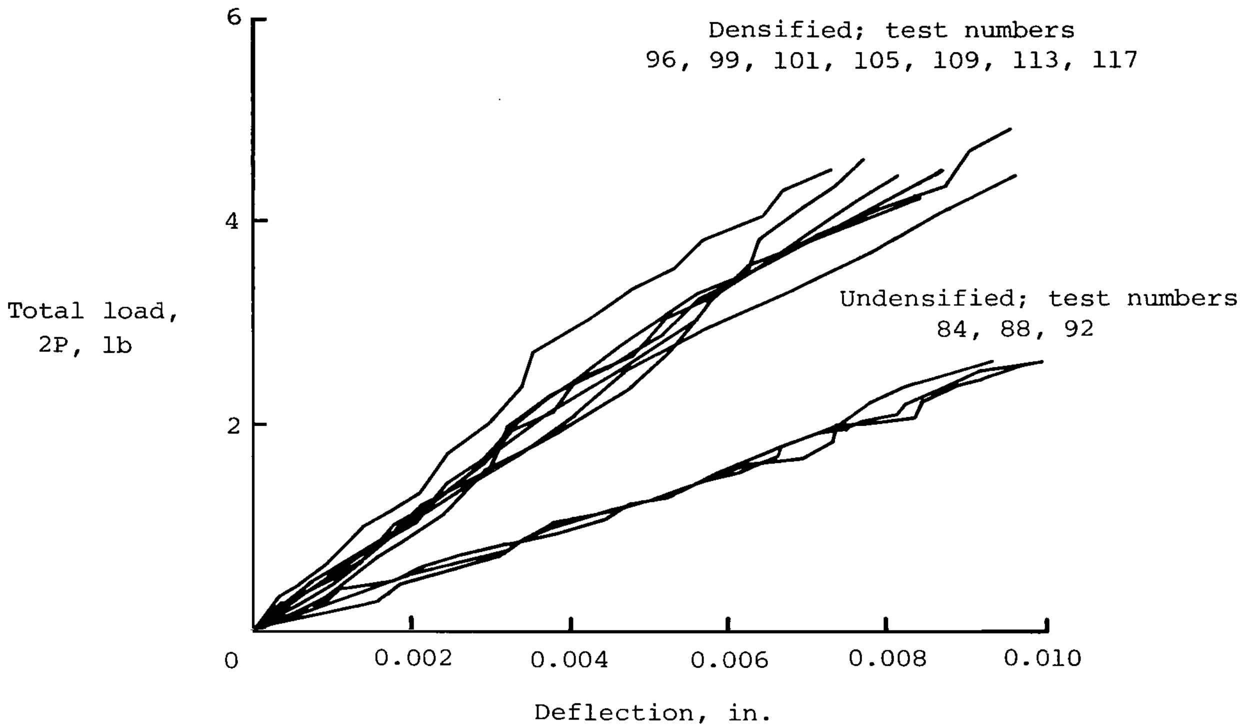

Figure 12.- Typical load-deflection results for densified and undensified LI-900 tile specimens.

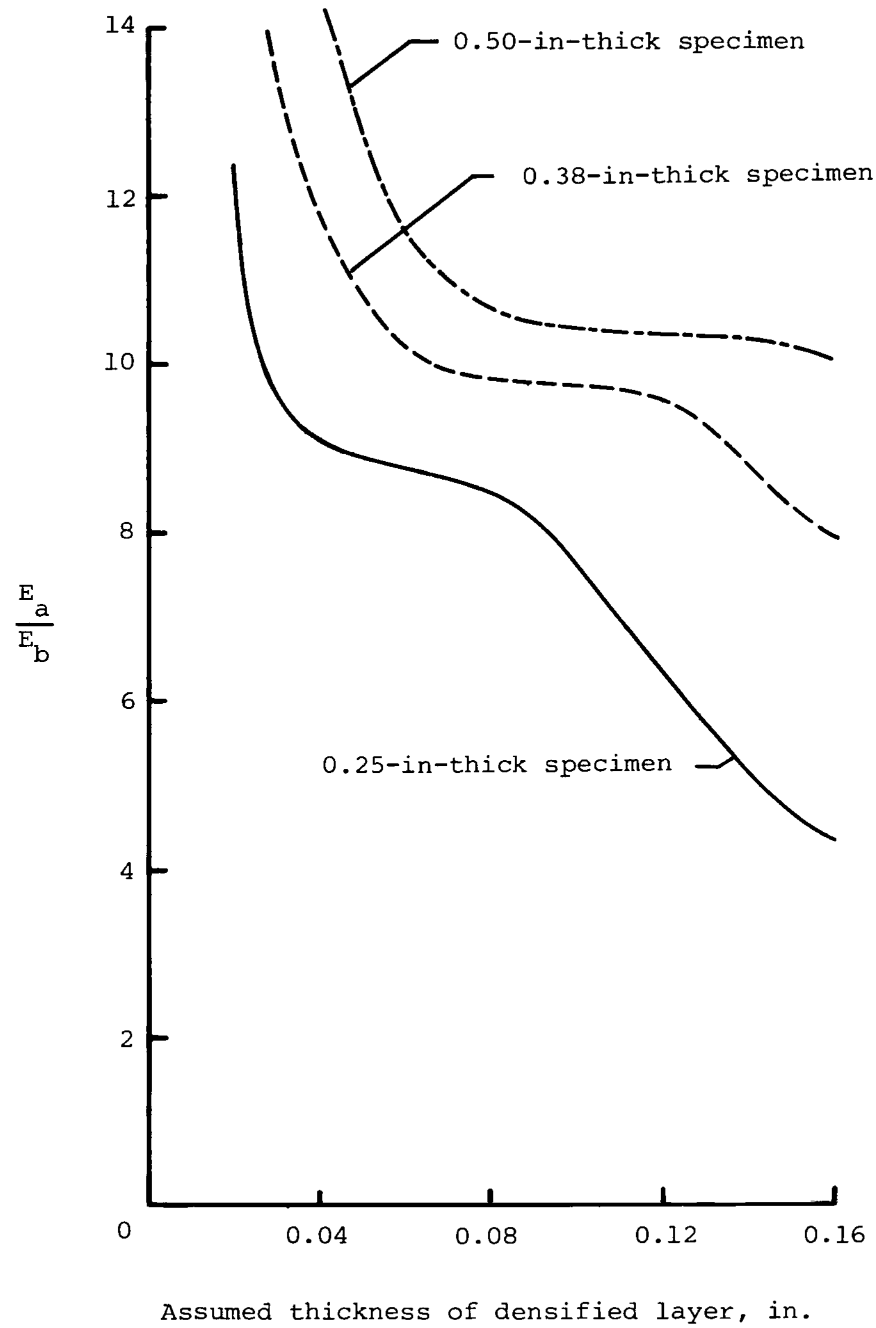

Figure 13.- Effect of assumed thickness of the densified layer on the calculated effective modulus for densified LI-900 tile material.

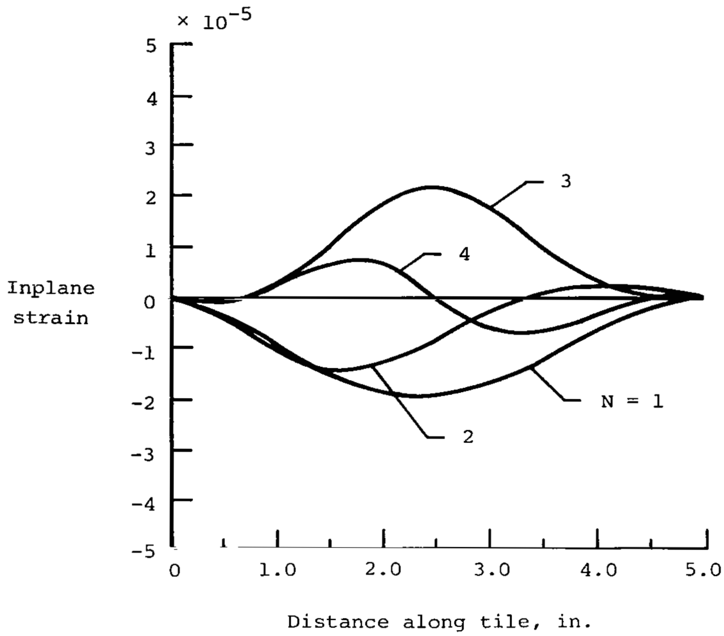

(a) Tile/SIP interface.

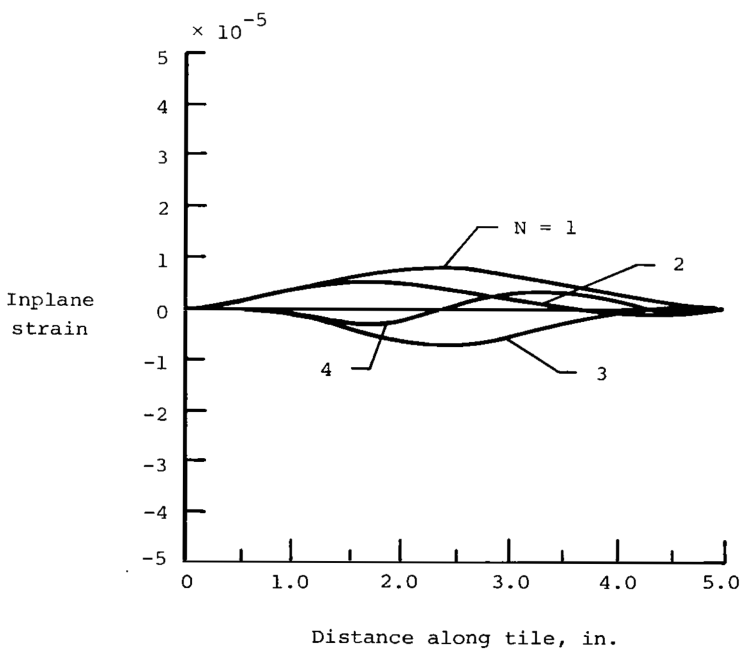

(b) Glass coating.

Figure 14.- Typical inplane strain distributions in undensified tile with substructure deformation and applied static loads representative of the highly loaded regions. N is the number of half-waves in the substructure.

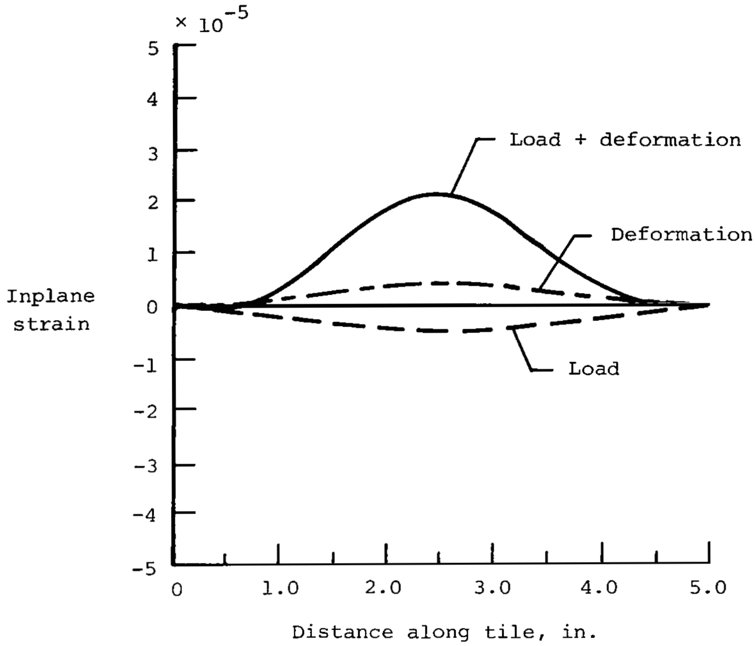

(a) Tile/SIP interface.

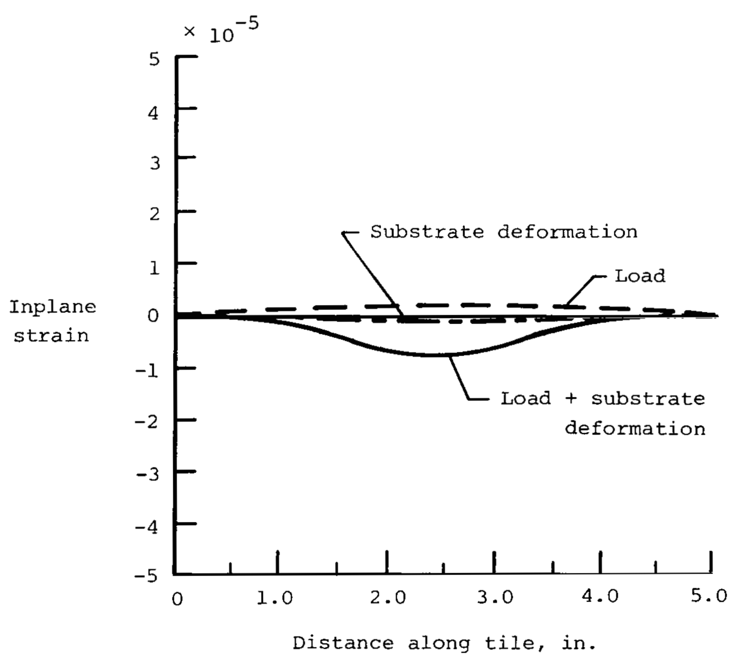

(b) Glass coating.

Figure 15.- Effects of static load and substructure deformation on maximum strain distribution in undensified tile. Substructure deformed in three half-waves.

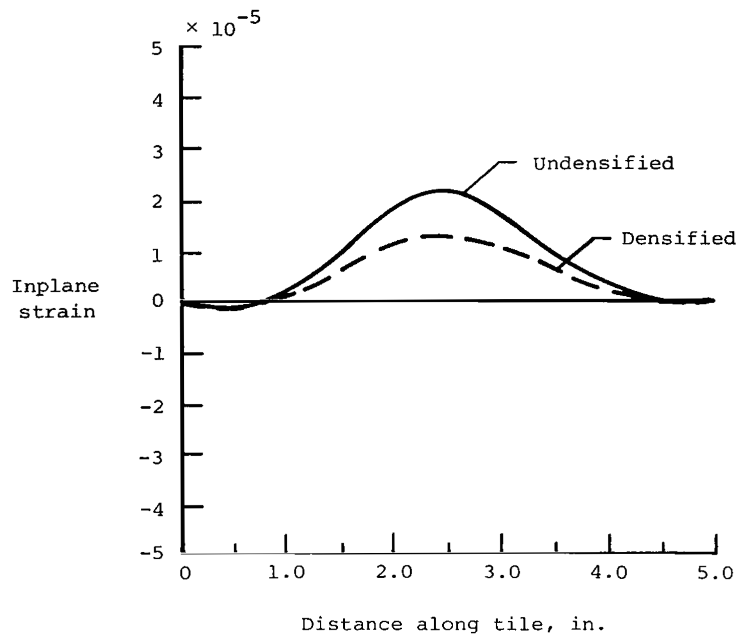

(a) Tile/SIP interface.

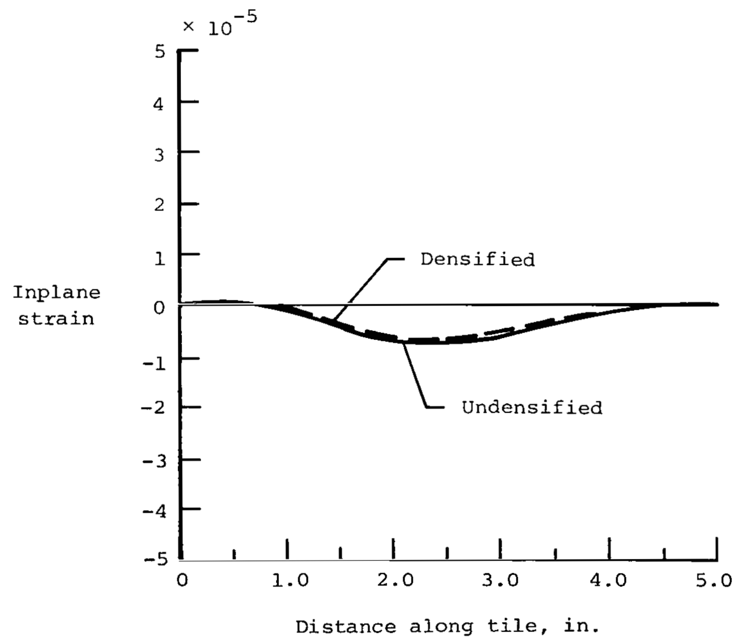

(b) Glass coating.

Figure 16.- Effect of densification on maximum strain distributions in tiles subjected to applied static loads representative of the highly loaded region and to substructure deformations.

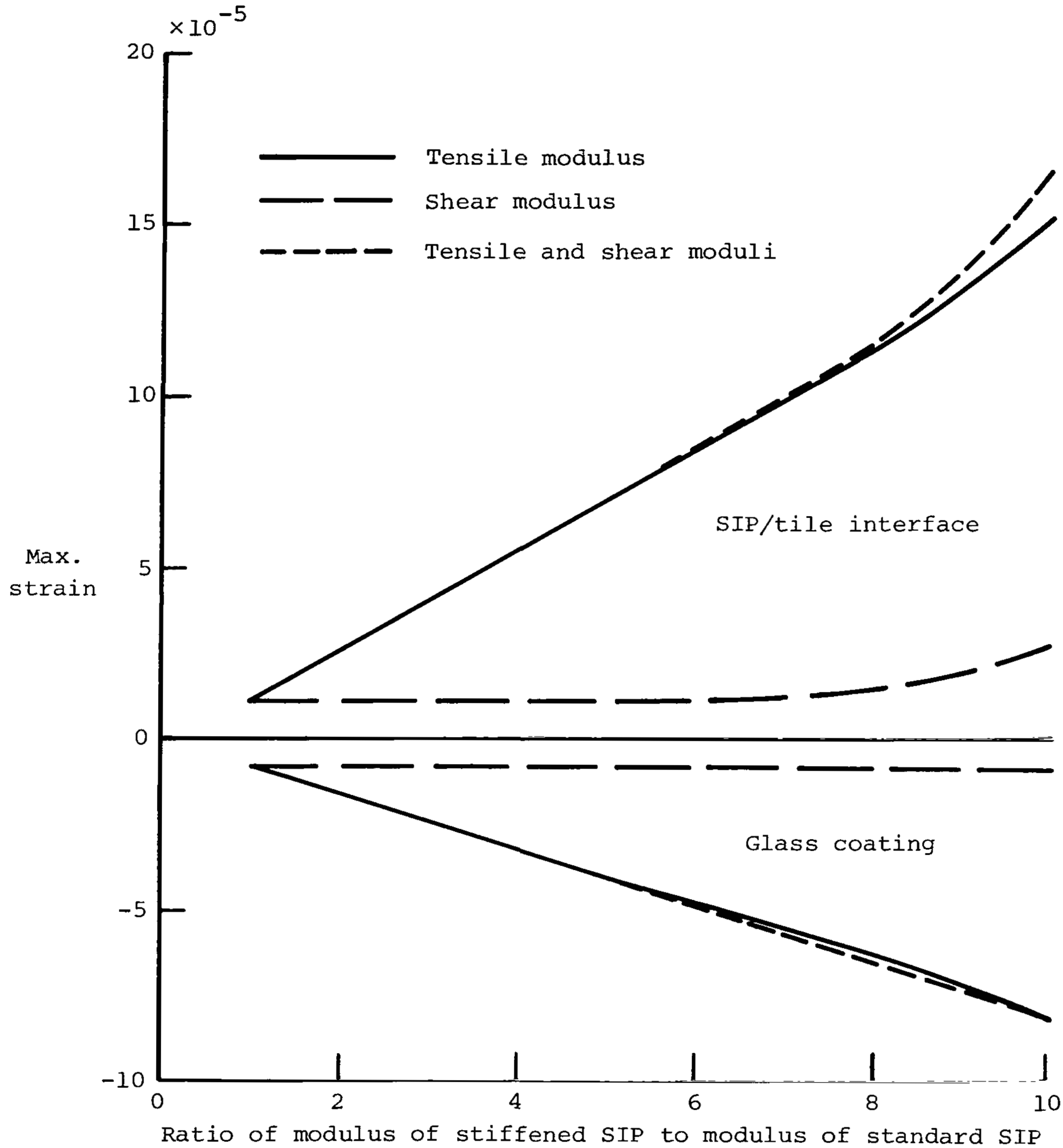

Figure 17.- Effect of SIP tensile and shear moduli on maximum inplane strain for 2.0-in-thick tile subjected to simulated flight static loads and substructure deformation.

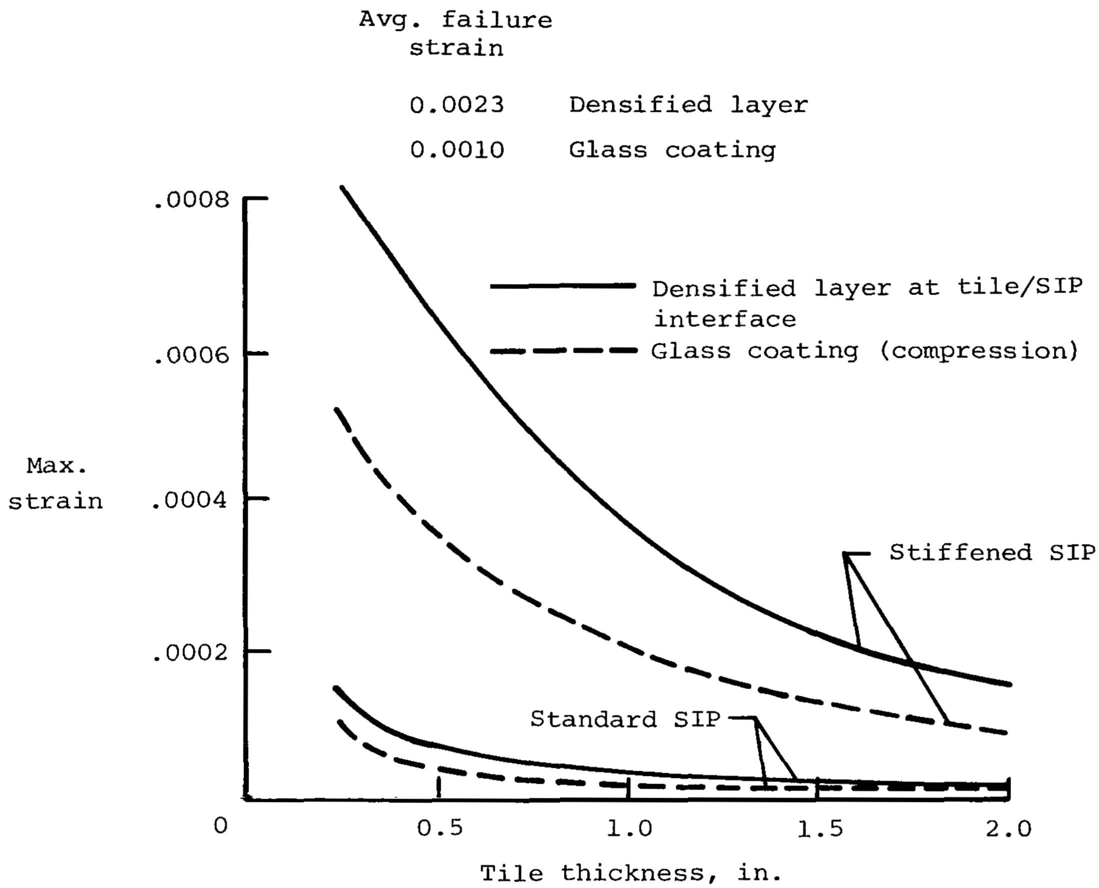

Figure 18.- Effect of tile thickness on maximum strain in Shuttle tiles mounted on standard and stiffened 0.160-in-thick SIP for loads and substructure deformations as defined in figure 1. Shear and tensile moduli of stiffened SIP are 10 times those of standard SIP.

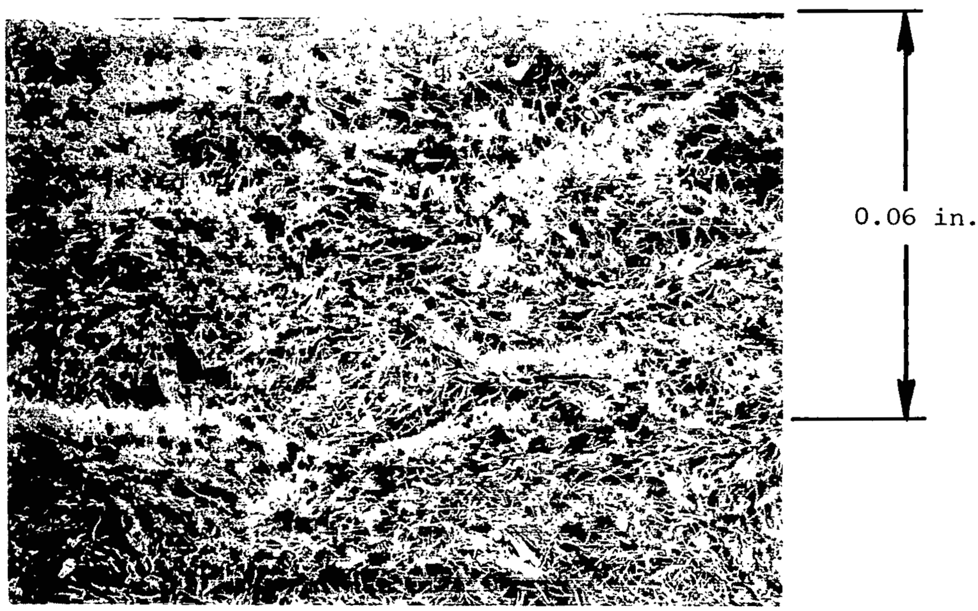

L-83-94

Figure 19.- Photomicrograph of typical cross section of densified LI-2200 tile specimen.

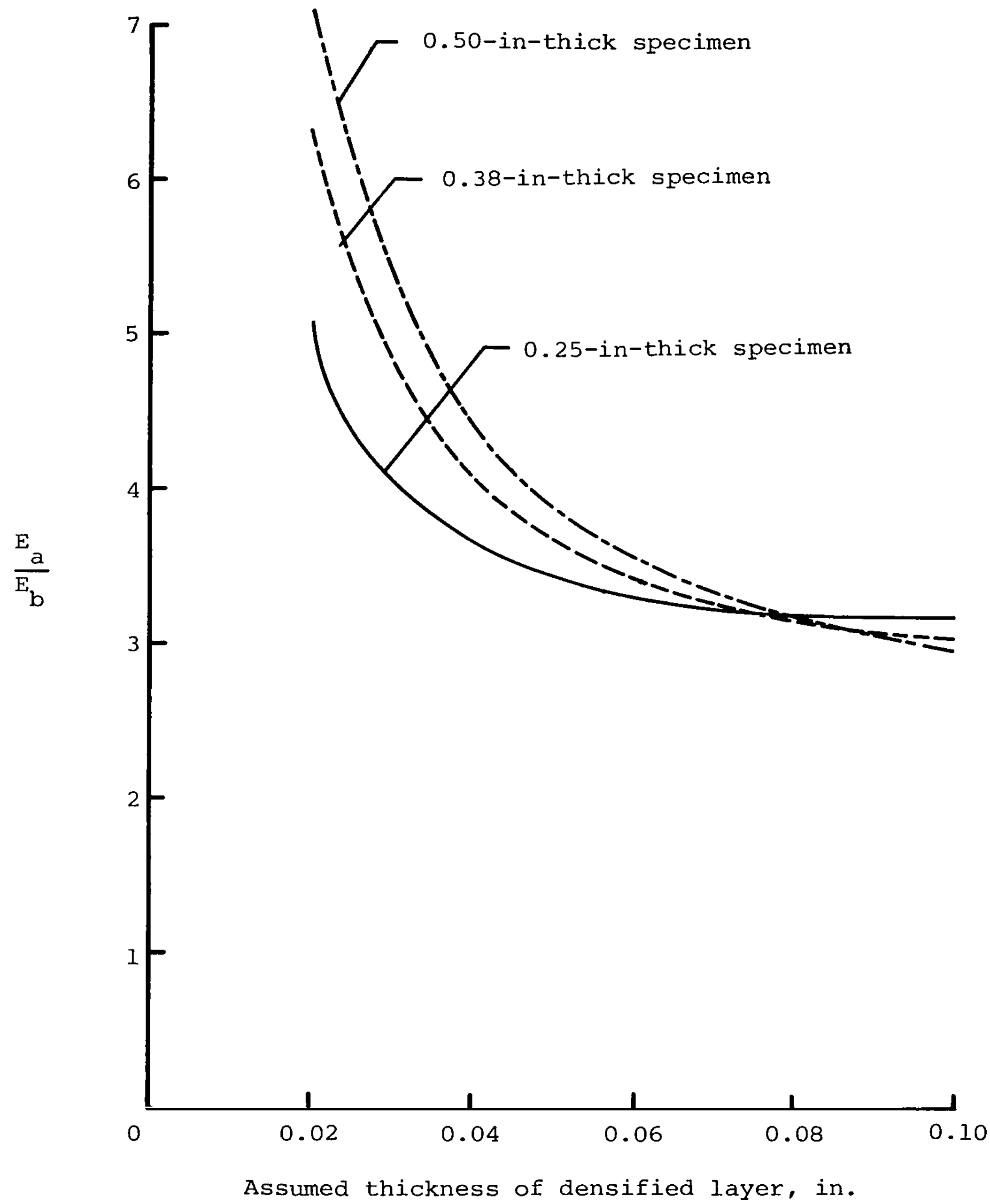

Figure 20.- Effect of assumed thickness of the densified layer on the calculated effective modulus for LI-2200 tile material.

1. Report No. NASA TP-2141	2. Government Accession No.	3. Recipient's Catalog No.
4. Title and Subtitle EFFECT OF STRAIN ISOLATOR PAD MODULUS ON INPLANE STRAIN IN SHUTTLE ORBITER THERMAL PROTECTION SYSTEM TILES		5. Report Date August 1983 6. Performing Organization Code 506-53-43-02
7. Author(s) James Wayne Sawyer		8. Performing Organization Report No. L-15575 10. Work Unit No.
9. Performing Organization Name and Address NASA Langley Research Center Hampton, VA 23665		11. Contract or Grant No.
12. Sponsoring Agency Name and Address National Aeronautics and Space Administration Washington, DC 20546		13. Type of Report and Period Covered Technical Paper 14. Sponsoring Agency Code
15. Supplementary Notes		

16. Abstract

An investigation was conducted on the thermal protection system used on the Space Shuttle orbiter to determine strains in the reusable surface insulation tiles under simulated flight loads. Also, the effects of changes in the strain isolator pad (SIP) moduli on the strains in the tile were evaluated. To analyze the SIP/tile system, it was necessary to conduct tests to determine inplane tension and compression modulus and inplane failure strain for the densified layer of the tiles. The test results show that densification of the LI-900 tile material increases the modulus by a factor of 6 to 10 and reduces the failure strain by about 50 percent. Analysis shows that the inplane strain levels in the Shuttle tiles in the highly loaded regions are approximately 2 orders of magnitude lower than the failure strain of the material. Calculations show that most of the LI-900 tiles on the Shuttle could be mounted on a SIP with tensile and shear stiffnesses 10 times those of the present SIP without inplane strain failure in the tile.

17. Key Words (Suggested by Author(s)) Thermal protection system Shuttle TPS Strain isolator pad Densified TPS	18. Distribution Statement Unclassified - Unlimited Subject Category 39

19. Security Classif. (of this report)	20. Security Classif. (of this page)	21. No. of Pages	22. Price
Unclassified	Unclassified	46	A03

For sale by the National Technical Information Service, Springfield, Virginia 22161

NASA-Langley, 1983